

1 **Assessing vegetation structure and ANPP dynamics in a** 2 **grassland-shrubland Chihuahuan ecotone using NDVI-** 3 **rainfall relationships**

4
5 **M. Moreno-de las Heras¹, R. Díaz-Sierra², L. Turnbull¹, J. Wainwright¹**

6 [1]{Department of Geography, Durham University, Durham DH1 3LE, United Kingdom }

7 [2]{Mathematical and Fluid Physics Department, Faculty of Sciences, UNED, Madrid 28040,
8 Spain }

9 Correspondence to: M. Moreno-de las Heras (mariano.moreno-de-las-heras@durham.ac.uk)

10 11 **Abstract**

12 Climate change and the widespread alteration of natural habitats are major drivers of
13 vegetation change in drylands. In the Chihuahuan Desert, large areas of grasslands dominated
14 by perennial grass species have transitioned over the last 150 years to shrublands dominated
15 by woody species, accompanied by accelerated water and wind erosion. Multiple mechanisms
16 drive the shrub-encroachment process, including precipitation variations, land-use change,
17 and soil erosion-vegetation feedbacks. In this study, using a simple ecohydrological
18 modelling framework, we show that herbaceous (grasses and forbs) and shrub vegetation in
19 drylands have different responses to antecedent precipitation due to functional differences in
20 plant growth and water-use patterns. Therefore, shrub encroachment may be reflected in the
21 analysis of landscape-scale vegetation-rainfall relationships. We analyze the structure and
22 dynamics of vegetation at an 18 km² grassland-shrubland ecotone in the northern edge of the
23 Chihuahuan Desert (McKenzie Flats, Sevilleta National Wildlife Refuge, NM, USA) by
24 investigating the relationship between decade-scale (2000-13) records of remotely sensed
25 vegetation greenness (MODIS NDVI) and antecedent rainfall. NDVI-rainfall relationships
26 show a high sensitivity to spatial variations on dominant vegetation types across the
27 grassland-shrubland ecotone, and provide ready biophysical criteria to (a) classify landscape
28 types as a function of the spatial distribution of dominant vegetation, and to (b) decompose
29 the NDVI signal into partial components of annual net primary production (ANPP) for

1 herbaceous vegetation and shrubs. Analysis of remote-sensed ANPP dynamics across the
2 study site indicates that plant growth for herbaceous vegetation is particularly synchronized
3 with monsoonal summer rainfall. For shrubs, ANPP is better explained by winter plus
4 summer precipitation, overlapping the monsoonal period (June to September) of rain
5 concentration. Our results suggest that shrub encroachment has not been particularly active in
6 this Chihuahuan ecotone for 2000-13. However, future changes in the amount and temporal
7 pattern of precipitation (i.e. reductions in monsoonal summer rainfall and/or increases in
8 winter precipitation) may enhance the shrub-encroachment process, particularly in the face of
9 expected upcoming increases in aridity for desert grasslands of the American Southwest.

10

11 **1 Introduction**

12 Land degradation is pervasive across many dryland regions, which cover over 40% of the
13 Earth's surface and account for about 30% of global terrestrial net primary productivity,
14 globally supporting about 2.5 billion inhabitants (Millennium Ecosystem Assessment, 2005).
15 Over recent decades these dryland regions have experienced growing human and climatic
16 pressures. The most dramatic landscape alterations resulting from these pressures are those
17 associated with desertification, which are perceived as catastrophic and largely irreversible
18 changes that can ultimately lead to relatively barren ecosystem states (Schlesinger et al.,
19 1990; Okin et al., 2009). A common form of vegetation change in drylands involves the
20 encroachment of desert shrub species into arid and semi-arid grasslands, which has already
21 affected more than 250 million hectares worldwide throughout the US, South America,
22 Southern Africa and Australia (D'Odorico et al., 2012; Turnbull et al., 2014).

23 A classic case of vegetation shift is the shrub-encroachment process that has been taking place
24 over the last 150 years in the Chihuahuan Desert in south-western USA and northern Mexico,
25 where large areas of grasslands dominated by C₄ perennial grass species (black grama,
26 *Bouteloua eriopoda*, and blue grama, *B. gracilis*) have been replaced by shrublands
27 dominated by C₃ desert shrub species (mainly creosotebush, *Larrea tridentata*, and honey
28 mesquite, *Prosopis glandulosa*). These changes in vegetation have been accompanied by
29 accelerated water and wind erosion (for example, Schlesinger et al., 1990; Wainwright et al.,
30 2000; Mueller et al., 2007; Turnbull et al., 2010a; Ravi et al., 2010). A complex range of
31 mechanisms have been suggested to explain the occurrence of this vegetation transition,
32 including external drivers that initiate the transition, and endogenous soil erosion-vegetation

1 feedbacks that further drive vegetation change (Turnbull et al., 2012). These internal
2 feedbacks strongly alter the organization and distribution of both vegetation and soil resources
3 (i.e. substrate, soil moisture and nutrients), strengthening the vegetation-change process (Okin
4 et al., 2009; Turnbull et al., 2010b, 2012; Stewart et al., 2014).

5 The onset of the grassland-shrubland transition in the Chihuahuan Desert is thought to have
6 started with the introduction of large numbers of domestic grazers, which may have favored
7 the establishment of pioneer shrubs via the creation of gaps (Buffington and Herbel, 1965;
8 van Auken, 2000; Webb et al., 2003) and via a reduction in the frequency and intensity of
9 natural wildfires (D'Odorico et al., 2012). Changing rainfall amount and frequency has also
10 been invoked as one of the major external drivers of shrub encroachment, which may
11 contribute to vegetation change by shifting competitive plant physiological advantages of
12 grass and desert shrub species (Gao and Reynolds, 2003; Snyder and Tartowsky, 2006;
13 Throop et al., 2012). However, there remains a lack of consensus regarding changes in rainfall
14 in the southwest USA over recent decades. Whilst Petrie et al. (2014) found no significant
15 changes in precipitation at the Sevilleta Long Term Ecological Research Site in central New
16 Mexico, other studies have reported significant increases in both annual and winter
17 precipitation at the Jornada Experimental Range in southern New Mexico, but concurrent
18 decreases in the size of discrete precipitation events (Wainwright, 2006; Turnbull et al.,
19 2013).

20 Comprehensive understanding of how desert grasslands are responding to the present
21 variability on both climate and land use is critical for environmental management, especially
22 in consideration of uncertainty regarding future climate change across many dryland regions.
23 Remote sensing of vegetation provides a valuable source of information for landscape
24 monitoring and forecasting of vegetation change in drylands (Okin and Roberts, 2004;
25 Pennington and Collins, 2007; Moreno-de las Heras et al., 2012). Satellite-derived
26 chlorophyll-sensitive vegetation indices, such as the Normalized Difference Vegetation Index
27 (NDVI), provide important information on vegetation structure (e.g. surface cover,
28 aboveground green biomass, vegetation type) and dynamics over broad spatial domains
29 (Anderson et al., 1993; Peters et al., 1997; Weiss et al., 2004; Pettorelli et al., 2005; Choler et
30 al., 2010; Forzieri et al., 2011).

31 In drylands, where vegetation dynamics are particularly well coupled with rainfall patterns,
32 the relationship between time series of NDVI and precipitation provides specific information

1 on the use of water for the production and maintenance of plant biomass (Pennington and
2 Collins, 2007; Notaro et al., 2010; Veron and Paruelo, 2010). Investigations of the
3 relationships between NDVI and rainfall suggest that arid and semi-arid vegetation responds
4 to antecedent (or preceding cumulative) precipitation rather than to immediate rainfall, since
5 plant growth is affected by the history of available soil moisture (Al-Bakri and Suleiman,
6 2004; Schwinning and Sala, 2004; Evans and Geerken, 2004; Moreno-de las Heras et al.,
7 2012). The length (or number of days) of antecedent rainfall that best explains the NDVI (or
8 green biomass) dynamics of dryland vegetation (hereafter optimal length of rainfall
9 accumulation, Olr) appears to be site-specific and strongly dependent on vegetation type
10 (Evans and Geerken, 2004; Prasad et al., 2007; Garcia et al., 2010). Herbaceous vegetation
11 (i.e. grass and forb life-forms) and shrubs usually show important differences in the patterns
12 of vegetation growth and water-use, which mediate the responses of plant biomass to rainfall
13 in drylands (Ogle and Reynolds, 2004; Gilad et al., 2007; Pennington and Collins, 2007;
14 Forzieri et al., 2011; Stewart et al., 2014). Thus, the study of the relationship between the
15 NDVI and rainfall may offer important clues for detecting broad-scale landscape changes
16 involving grassland-shrubland transitions in arid and semi-arid landscapes.

17 The aim of this study is to analyze vegetation structure and dynamics at a Chihuahuan
18 grassland-shrubland ecotone (McKenzie Flats, Sevilleta National Wildlife Refuge, New
19 Mexico, USA). To fulfil this aim we explore the relationship between decade-scale (2000-13)
20 records of remote-sensed vegetation greenness (MODIS NDVI) and rainfall. Our analysis is
21 based on a new approach that examines characteristic NDVI-rainfall relationships for
22 dominant vegetation types (i.e. herbaceous vegetation and woody shrubs) to investigate the
23 organization and dynamics of vegetation as a way of evaluating how the shrub-encroachment
24 process occurs.

25 This paper is organized in two parts. First, we present the conceptual underpinning and
26 theoretical basis of our study, by using a simple, process-based ecohydrological model to
27 illustrate the biophysical control of the relationship between plant biomass dynamics and
28 antecedent rainfall for dryland herbaceous and shrub vegetation. Secondly, we empirically
29 determine reference optimal lengths of rainfall accumulation (in days) for herbaceous and
30 shrub vegetation (Olr_{hv} and Olr_s) in a 18 km² Chihuahuan ecotone, and use these vegetation-
31 type specific NDVI-rainfall metrics to (i) analyze the spatial organization and dynamics of net
32 primary production (NPP) for herbaceous vegetation and shrubs, and to (ii) explore the impact

1 of inter-annual variations in seasonal rainfall on the dynamics of vegetation production at the
2 grassland-shrubland ecotone.

3

4 **2 Theoretical basis: herbaceous and shrub plant biomass-rainfall** 5 **relationships in drylands**

6 Dryland herbaceous vegetation (i.e. grass and forb life-forms) and shrubs usually exhibit
7 important differences in the patterns of vegetation growth and water-use. Herbaceous
8 vegetation typically shows quick and intense growth pulses synchronized with major rainfall
9 events, while the dynamics of plant biomass for shrubs is generally less variable in time
10 (Sparrow et al., 1997; Lu et al., 2003; Garcia et al., 2010). These dissimilar growth responses
11 are controlled biophysically by the different plant growth and mortality rates associated with
12 herbaceous vegetation and shrubs. While grasses and forbs are associated with high rates of
13 plant growth and mortality, shrubs are associated with comparatively lower plant growth and
14 mortality rates (Ogle and Reynolds, 2004; Gilad et al., 2007).

15 We use a simplified version of the dynamic ecohydrological model developed by Rietkerk et
16 al. (2002) to illustrate conceptually how the vegetation-specific rates of plant growth and
17 mortality control the relationship between the dynamics of aboveground biomass and
18 antecedent rainfall for herbaceous vegetation and shrubs in drylands. The model consists of
19 two interrelated differential equations; one describing the dynamics of vegetation
20 (aboveground green biomass, B , g m^{-2}) and the other describing soil-moisture dynamics (soil-
21 water availability, W , mm).

22 Changes in plant biomass are controlled by plant growth and mortality:

$$23 \frac{dB}{dt} = g_{max} \frac{W-W_0}{W+k_w} B - mB, \quad (1)$$

24 where plant growth is a saturation function of soil-moisture availability, and is determined by
25 the maximum specific plant-growth rate (g_{max} , day^{-1}), the permanent wilting point or
26 minimum availability of soil moisture for vegetation growth (W_0 , mm), and a half saturation
27 constant (k_w , mm). Plant senescence (biomass loss) is controlled by a plant-specific mortality
28 coefficient (m , day^{-1}).

29 Soil-water dynamics are controlled by rainfall infiltration, plant transpiration, and soil-
30 moisture loss due to both deep drainage and direct evaporation:

$$1 \quad \frac{dW}{dt} = P \frac{B+k_i \cdot i_0}{B+k_i} - c g_{max} \frac{W-W_0}{W+k_w} B - r_w W, \quad (2)$$

2 where water infiltration is modelled as a saturation function of plant biomass, characterized
 3 by the minimum proportion of rainfall infiltration in the absence of vegetation (i_0 ,
 4 dimensionless), a half saturation constant (k_i , g m^{-2}) and daily precipitation (P , mm day^{-1}).
 5 Plant transpiration is controlled by plant growth, and is modulated by a plant-water-
 6 consumption coefficient (c , l g^{-1}). Finally, water losses to both deep drainage and direct
 7 evaporation are modeled as a linear function of soil-water availability, with a rate r_w (day^{-1}).
 8 A Maple 9.5 (Maplesoft, Waterloo, Canada) code for this model is available for download as
 9 online supporting material of this article (Code 1).

10 Two sets of plant-growth and mortality coefficients were applied to this model to simulate
 11 vegetation dynamics for a herbaceous species ($g_{max}=0.32 \text{ day}^{-1}$, $m=0.05 \text{ day}^{-1}$) and a shrub
 12 ($g_{max}=0.12 \text{ day}^{-1}$, $m=0.03 \text{ day}^{-1}$), following criteria established in previous studies (Ogle and
 13 Reynolds, 2004; Gilad et al., 2007). Plant-biomass dynamics for these two vegetation types
 14 (Fig. 1a) were modelled using a north Chihuahuan Desert 15-year daily precipitation series
 15 obtained at the Sevilleta National Wildlife Refuge (Sevilleta LTER,
 16 <http://sev.lternet.edu/data/sev-1>; mean annual rainfall 238 mm) and a set of parameters
 17 obtained from literature suited to dryland environments: $W_0=0.05 \text{ mm}$, $k_w=0.45 \text{ mm}$,
 18 $k_i=180 \text{ g m}^{-2}$, $i_0=0.20$, $c=0.1 \text{ l g}^{-1}$, $r_w=0.1 \text{ day}^{-1}$ (Rietkerk et al., 2002; Gilad et al., 2007;
 19 Saco and Moreno-de las Heras, 2013).

20 Using this model, we explored the strength of the plant biomass-precipitation relationship as a
 21 function of the length of rainfall accumulation (Fig 1b). We have applied Pearson's R
 22 correlation between the simulated plant biomass for both the herbaceous and the shrub species
 23 and antecedent rainfall series using various lengths of rainfall accumulation; i.e. for any time
 24 t_i in the plant biomass series, the rainfall in the preceding day (t_{i-1}), the cumulative rainfall in
 25 the two preceding days ($t_{i-1:i-2}$), in the three preceding days ($t_{i-1:i-3}$) and so on. Modelling
 26 results show that the plant biomass-rainfall correlation is maximized at 52 days of cumulative
 27 rainfall for the simulated herbaceous species ($Ol_{r_{hv}}=52 \text{ days}$) and is maximized at 104 days
 28 of cumulative rainfall for the modeled shrub species ($Ol_{r_s}=104 \text{ days}$; Fig. 1b). This result
 29 indicates that the simulated herbaceous species responds to short-term (~ two months)
 30 antecedent rainfall for the production of plant biomass whilst the simulated shrub species
 31 responds to a longer period of antecedent precipitation to support plant dynamics. Here,

1 $ARain_{hv}$ and $ARain_s$ are defined as the antecedent rainfall series that optimize those
2 vegetation-type specific relationships (i.e. time series of precedent rainfall with accumulation
3 lengths Olr_{hv} for herbaceous vegetation and Olr_s for shrubs, Fig. 1a). Further analysis using a
4 range of plausible values for the plant-mortality and maximum plant-growth coefficients (Fig.
5 1c) indicates that Olr increases largely by reducing the characteristic plant-mortality and
6 growth rates of vegetation, and therefore suggests a strong influence on vegetation type.
7 Sensitivity analysis of Olr to other model parameters (Supplementary Fig.1 in the online
8 supporting information of this study) indicates that W_0 , k_w , k_i , and c have negligible effects on
9 simulated Olr values. Reductions on bare soil infiltration (i_0) and increases on water loss by
10 direct evaporation and/or deep drainage (r_w) can impact Olr_{hv} and Olr_s values, ultimately
11 amplifying the differences we obtained between vegetation types. Other factors not explicitly
12 considered in our model, such as differences in root structure, may also reinforce herbaceous
13 and shrub differences in time-scale plant responses to antecedent precipitation (Reynolds et
14 al., 2004; Collins et al., 2014).

15 The simple model presented in this study provides a good starting point for addressing general
16 differences in plant responses to antecedent precipitation for different vegetation types in
17 drylands. Overall, our modelling results illustrate conceptually the distinct dependence of the
18 relationship between plant biomass and antecedent precipitation on vegetation type,
19 particularly when comparing the dynamics of dryland herbaceous and shrub vegetation.

20 In the following part of this study, we empirically determine and use metrics of reference
21 vegetation-type specific relationships between aboveground green biomass and antecedent
22 rainfall (i.e. optimal Olr_{hv} and Olr_s lengths, and corresponding $ARain_{hv}$ and $ARain_s$ series) to
23 explore the spatial organization and NPP dynamics of herbaceous and shrub vegetation at a
24 semi-arid grassland-shrubland ecotone.

25

26 **3 Materials and methods**

27 **3.1 Study area**

28 This study is conducted in the Sevilleta National Wildlife Refuge (SNWR), central New
29 Mexico, USA, the location of the Sevilleta Long Term Ecological Research (LTER) site. The
30 SNWR is located in the northern edge of the Chihuahuan Desert, and is a transition zone
31 between four major biomes: the Chihuahuan Desert, the Great Plains grasslands, the Colorado

1 Plateau steppe, and the Mogollon coniferous woodland (Fig. 2a). Livestock grazing has been
2 excluded from the SNWR since 1973, following 40 years of rangeland use. Due to the biome-
3 transition nature of the SNWR, minor variations in environmental conditions and/or human
4 use can result in large changes in vegetation composition and distribution at the refuge
5 (Turnbull et al., 2010b). Analysis of aerial photographs and soil-carbon isotopes indicate that
6 the extent of desert shrublands has considerably increased over the grasslands in regions of
7 the SNWR over the last 80 years (Gosz, 1992; Turnbull et al., 2008).

8 Our study area is an 18 km² grassland-shrubland ecotone within the McKenzie Flats, an area
9 of gently sloping terrain on the eastern side of the SNWR (Fig. 2b). This study area extends
10 over two LTER Core Sites established in 1999 (Fig. 2c): a desert shrubland (Creosotebush
11 SEV LTER Core Site) dominated by creosotebush, and a grassland (Black Grama SEV LTER
12 Core Site) dominated by black grama. The central and northeastern parts of the study area are
13 mixed black and blue grama (*Bouteloua eriopoda* and *B. gracilis*, respectively) grasslands.
14 The abundance of creosotebush (*Larrea tridentata*) in the grasslands is generally low,
15 although smaller shrubs and succulents (e.g. *Gutierrezia sarothrae*, *Ephedra torreyana*, *Yucca*
16 *glauca*, *Opuntia phaeacantha*) can be common. The abundance of perennial grass species
17 decreases to the southern and southwestern parts of the study area, where creosotebush stands
18 are widely distributed with in general low (although variable in time) amounts of annual forbs
19 and grasses. Soils are Turney sandy loams (Soil Survey Staff, 2010) with about 60% sand and
20 20% silt content (Muldavin et al., 2008; Turnbull et al., 2010b). The climate is semi-arid, with
21 mean annual precipitation of ~240 mm that is made up of 57% falling in the form of high-
22 intensity convective thunderstorms during the summer monsoon (June to September) and the
23 remainder being received as low-intensity frontal rainfall and snow (October to May). Mean
24 annual daily temperature is 14°C, with a winter average of 6°C and a summer average of
25 24°C. Daily air temperature rises over 10°C in the beginning of April, leading to the onset of
26 the yearly cycles of vegetation growth (Weiss et al., 2004). Vegetation growth in the study
27 area generally peaks between July and September, coinciding with the summer monsoon
28 (Muldavin et al., 2008).

29 **3.2 Vegetation measurements (remote sensed and ground based) and rainfall** 30 **data**

31 We use temporal series of NDVI as a proxy of aboveground green biomass in our study area.
32 NDVI is a remote-sensed chlorophyll-sensitive vegetation index that correlates with green

1 biomass in semi-arid environments (Anderson et al., 1993; Huete et al., 2002; Veron and
2 Paruelo, 2010). Differences in soil background brightness can generate important
3 uncertainties in relating NDVI levels to dryland vegetation, especially when vegetation cover
4 is low and soil type is heterogeneous in space (Okin et al., 2001). Despite these uncertainties,
5 multiple studies have demonstrated the usefulness of NDVI for examining primary production
6 and vegetation structure in arid and semi-arid ecosystems (for example, Weiss et al., 2004;
7 Choler et al., 2010; Moreno-de las Heras et al., 2012), and particularly in Chihuahuan
8 landscapes with sparse vegetation (30-50% cover) similar to those included in this study
9 (Peters and Eve, 1995; Peters et al., 1997; Pennington and Collins, 2007; Notaro et al., 2010).
10 We compiled decade-scale (2000-13) series of NDVI with a 16-day compositing period from
11 the MODIS Terra satellite (MOD13Q1 product, collection 5, approx. 250 m resolution). We
12 used the NASA Reverb search tool (NASA EOSDIS, <http://reverb.echo.nasa.gov/>) to
13 download the corresponding MODIS tiles. The data were re-projected to UTM WGS84 and
14 further resampled to fit our 18-km² study area (335 pixels; 231.5 m pixel resolution after re-
15 projection to UTM coordinates). We checked the reliability layer of the acquired MODIS
16 products and discarded those NDVI values that did not have the highest quality flag value
17 (less than 1 % of data). Missing values were interpolated using a second order polynomial. To
18 reduce inherent noise, the NDVI time series were then filtered by applying a Savitzky-Golay
19 smoothing algorithm, as recommended by Choler et al. (2010).

20 To validate remote sensing analysis of the spatial distribution of vegetation types, the
21 dominance of herbaceous vegetation, shrubs, perennial grass, forbs, and creosotebush plants
22 was recorded at a set of 27 control points (Fig. 2c) using the point-intercept method (Godin-
23 Alvarez et al., 2009). Vegetation presence/absence of the aforementioned vegetation types
24 was recorded every metre using a 2-cm diameter, 1.2-m tall, metal rod pointer along five 50-
25 m long linear transects that were laid at each control point at random directions (without
26 overlapping). Dominance was determined as the relative abundance of a particular vegetation
27 type in relation to the total amount of vegetated points found per linear transect.

28 Reference information on aboveground net primary production (NPP) was obtained from a
29 pre-existing, decade-scale (2000-11) dataset (Sevilleta LTER, <http://sev.lternet.edu/data/sev-182>). This dataset was recorded in a set of 10 sampling webs distributed within the Black
30 Grama and Creosotebush SEV LTER Core Sites (five webs per Core Site, Fig. 2c). Each
31 sampling web consisted of four 25-m² square sub-plots located in each cardinal direction
32

1 around the perimeter of a 200-m diameter circle, with four 1-m² quadrats spatially distributed
2 in the internal corners of the 25-m² sub-plots. A detailed description of the methods that were
3 applied for the development of the SEV LTER field NPP dataset can be found in Muldavin et
4 al. (2008). Briefly, species-specific plant standing biomass was estimated three times per year
5 (in February-March, May-June and September-October) using allometric equations, and NPP
6 was calculated seasonally for spring (the difference in plant biomass from March to May),
7 summer (from June to September), and fall/winter (from October to February). For this study,
8 we have used lumped records of annual net primary production (ANPP) for herbaceous
9 vegetation and shrubs that were spatially averaged at the Core Site scale. ANPP for each
10 yearly cycle of vegetation growth has been calculated as the sum of the seasonal NPP records
11 (i.e. spring + summer + fall/winter).

12 Daily rainfall information for this study was obtained from an automated meteorological
13 station located in the study site (the Five Points weather station, SEV LTER, Fig. 2c; Sevilleta
14 LTER, <http://sev.lternet.edu/data/sev-1>). The meteorological station is equipped with a rain
15 gauge that records precipitation on a 1-minute basis during periods of rain.

16 **3.3 Reference NDVI-rainfall metrics for herbaceous vegetation and shrubs**

17 We explored reference NDVI-rainfall relationships for herbaceous vegetation and shrubs in
18 the Black Grama and Creosotebush SEV LTER Core Sites (where vegetation is dominantly
19 herbaceous and shrub, respectively) using the 2000-13 NDVI time series (averaged from five
20 MODIS pixels in each site, covering a total of 1200 m² per site). Pearson's correlations
21 between NDVI and antecedent precipitation series were calculated for the two sites using
22 various lengths of rainfall accumulation (1-300 days). Optimal length of rainfall accumulation
23 for herbaceous vegetation and shrubs (Olr_{hv} and Olr_s , respectively) were then determined as
24 the length of rainfall accumulation (in days) of the antecedent precipitation series that
25 maximized the correlations between NDVI and rainfall in the black grama- and the
26 creosotebush-dominated Core Sites, respectively. Growth of non-dominant herbaceous
27 vegetation in arid shrublands can make the detection of shrub-specific NDVI-rainfall metrics
28 (i.e. Olr_s) difficult due to the emergence of secondary Olr_{hv} values, particularly in wet years
29 with strong herbaceous production (Moreno-de las Heras et al., 2012). We applied detailed
30 analysis of the NDVI-rainfall relationships in the Core Sites for each annual cycle of
31 vegetation growth to facilitate discrimination of the Olr_{hv} and Olr_s metrics. Our approach
32 assumes linearity between rainfall and both NDVI values and green biomass, which has been

1 broadly demonstrated to occur for dryland vegetation (Evans and Geerken, 2004; Choler et
2 al., 2010; Notaro et al., 2010; Veron and Paruelo, 2010; Moreno-de las Heras et al., 2012) and
3 particularly in our grassland-shrubland desert ecotone (Pennington and Collins, 2007;
4 Muldavin et al., 2008).

5 The optimal antecedent rainfall series determined in the Core Sites for herbaceous vegetation
6 ($ARain_{hs}$, with Olr_{hv} length of rainfall accumulation) and shrubs ($ARain_s$, with Olr_s rainfall
7 accumulation length) were further used in our 18-km² ecotone to classify landscape types and
8 to decompose local NDVI signals into greenness components for herbaceous and shrub
9 vegetation.

10 **3.4 Spatial distribution of vegetation types and landscape classification**

11 We applied analysis of the relationship between local series of NDVI and the reference
12 $ARain_{hv}$ and $ARain_s$ antecedent rainfall series to determine the spatial distribution of dominant
13 vegetation and classify landscape types over our 18-km² ecotone study area. This analysis
14 builds on the assumption that spatial variations in the NDVI-rainfall relationship reflect
15 spatial differences in the dominance of vegetation types. We assume that areas dominated by
16 herbaceous vegetation (or shrubs) will show a strong NDVI-rainfall relationship for the
17 herbaceous-characteristic $ARain_{hv}$ (or the shrub-characteristic $ARain_s$) antecedent rainfall
18 series along the study period.

19 The strength of the relationship between NDVI and rainfall (quantified using Pearson's R
20 correlation between NDVI and antecedent precipitation) was calculated for every MODIS
21 pixel in the study area using the reference $ARain_{hv}$ and $ARain_s$ antecedent rainfall series.
22 Correlation values were determined for each cycle of vegetation growth (April-March) in
23 2000-13. In order to reduce data dimensionality, we applied Principal Component Analysis
24 (PCA) using the calculated correlation coefficients as variables for analysis (28 variables
25 resulting from the two vegetation-specific antecedent rainfall series and the 14 growing
26 cycles). We studied further the relationship between the main PCA factors and ground-based
27 dominance of vegetation types using the reference vegetation distribution dataset (27 control
28 points). Finally, we used the empirical relationships between vegetation dominance and the
29 main PCA factors to discriminate differentiated landscape types across the study area: grass-
30 dominated (GD), grass-transition (GT), shrub-transition (ST) and shrub-dominated (SD)
31 landscapes.

3.5 NDVI decomposition and transformation into herbaceous and shrub ANPP components

Time series of NDVI at any specific location reflects additive contributions of background soil and the herbaceous and woody shrub components of vegetation (C_{bs} , C_{hv} , and C_s , respectively) for that particular site (Lu et al., 2003):

$$NDVI(t) = C_{bs}(t) + C_{hv}(t) + C_s(t), \quad (3)$$

Montandon and Small (2008) carried out *in situ* measurements of field spectra convolved by the MODIS bands to determine the background soil contribution to NDVI in the SNWR. They obtained a soil NDVI value of 0.12 for Turney sandy loam soils, which are broadly distributed across the McKenzie Flats. Analysis of the local MODIS NDVI time series revealed that this soil-background reference value broadly matches the minimum NDVI values for our study area. Application of reference soil values in NDVI decomposition and normalization methodologies provides an efficient standardization approach for characterizing the background soil baseline, particularly in areas with homogeneous soils (Carlson and Ripley, 1997; Roderick et al., 1999; Lu et al., 2003; Choler et al. 2010). Soil background NDVI may change with soil-moisture content (Okin et al., 2001). Although this effect can be especially important for dark organic-rich soils, soil-moisture variations have shown a little impact in desert-type bright sandy and sandy-loam soils, as those represented in the study area (Huete et al., 1985). Therefore, a constant value of 0.12 was applied to subtract the background soil baseline (C_{bs}) from the NDVI time series, obtaining a new set of soil-free series ($NDVI_O$):

$$NDVI_O(t) = C_{hv}(t) + C_s(t), \quad (4)$$

We applied the reference herbaceous- and shrub-characteristic antecedent rainfall series, $ARain_{hv}$ and $ARain_s$, to partition single time series of soil-free NDVI ($NDVI_O$) into separate contributions for herbaceous vegetation (C_{hv}) and woody shrubs (C_s) across our study area. This approach is based on the assumption that the primary determinant of the dynamics of both NDVI and green biomass in Chihuahuan landscapes is the rainfall pattern (Huenneke et al., 2002; Weiss et al., 2004; Muldavin et al., 2008; Pennington and Collins, 2007; Notaro et al., 2010; Forzieri et al., 2011), and therefore the partial contributions of herbaceous vegetation and shrubs to NDVI can be estimated as a function of their characteristic dependency on antecedent rainfall. In other words, we assume that C_{hv} and C_s for any t_i are

1 proportional to $ARain_{hv}$ and $ARain_s$. The NDVI components for herbaceous vegetation and
2 shrubs were partitioned using the following two-step NDVI-decomposition procedure (Maple
3 9.5 code for analysis provided as online supporting material of this article; Code 2).

4 First, we applied first-order least-squares optimization of the relationship between soil-free
5 NDVI ($NDVI_O$) and the vegetation-type specific antecedent rainfall series ($ARain_{hv}$ and
6 $ARain_s$ for herbaceous vegetation and shrub, respectively):

$$7 \quad NDVI_O(t) = h ARain_{hv}(t) + s ARain_s(t), \quad (5)$$

8 where, h and s represent vegetation-type specific rainfall-NDVI conversion coefficients for
9 the herbaceous and shrub components.

10 Secondly, we used the determined coefficients h and s to calculate the weights of C_{hv} and C_s
11 on the time series (i.e. the predicted percentage contribution of each vegetation type over the
12 predicted totals for any t_i). Seasonal variations in other environmental factors (e.g.
13 temperature, day length) may influence NDVI dynamics for Chihuahuan vegetation, shaping
14 the responses of vegetation to precipitation (Weiss et al., 2004; Notaro et al., 2010). In order
15 to preserve the observed seasonality of the original NDVI time series in the decomposed
16 signals for herbaceous and shrub vegetation, the predicted weights (or percentage
17 contributions) of the fitted vegetation components were reassigned to the NDVI levels of the
18 original time series, obtaining the final NDVI components for herbaceous vegetation and
19 shrubs (C_{hv} , and C_s , respectively).

20 The 2000-13 time series of NDVI were decomposed into separate contributions of herbaceous
21 vegetation and shrubs for the Black Grama and Cresotebush SEV LTER Core Sites. We used
22 the reference 2000-11 field NPP dataset to study the relationship between the decomposed
23 NDVI time series and ground-based estimates of herbaceous and shrub NPP for the Core
24 Sites. The sum of the herbaceous and the shrub NDVI components ($\sum NDVI_{veg.type}$) were
25 calculated for each growing cycle of vegetation (April-March). We further determined the
26 relationships between field ANPP estimates of herbaceous and shrub vegetation and
27 $\sum NDVI_{veg.type}$. Finally, we applied the signal-decomposition procedure to every single NDVI
28 time series of the 335 MODIS pixels contained within our study area. The established Core
29 Site NDVI-ANPP relationships were used to estimate herbaceous and shrub ANPP across the
30 18 km² study site.

3.6 Spatiotemporal dynamics of vegetation production and impact of seasonal precipitation on herbaceous and shrub ANPP

We used the remotely sensed ANPP estimations and landscape-type classification (GD, grass-dominated, GT, grass-transition, ST, shrub-transition, and SD, shrub-dominated landscapes) to analyze the spatiotemporal dynamics of ANPP along our study grassland-shrubland ecotone, applying repeated-measures ANOVA with time as within subjects factor and landscape type as between subjects factor. Departures from sphericity were corrected using the Greenhouse-Geisser F-ratio method for repeated-measures ANOVA (Girden, 1992). 2000-13 activity of the shrub-encroachment phenomenon for the established landscape types (GD, GT, ST and SD) was explored applying Pearson's *R* correlation between shrub contribution to total ANPP and time.

We used three different seasonal precipitation metrics to analyze the impact of inter-annual variations in seasonal precipitation on the production of herbaceous and shrub vegetation at our ecotone: (i) preceding non-monsoonal rainfall ($Rain_{PNM}$, from October to May) that takes place before the summer peak of vegetation growth, (ii) summer monsoonal precipitation ($Rain_{SM}$, from June to September), and (iii) late non-monsoonal rainfall ($Rain_{LNM}$, from October to March) that takes place at the end of the annual cycles of vegetation growth. The effects of seasonal precipitation on herbaceous and shrub ANPP for the established landscape types (grass-dominated, grass-transition, shrub-transition and shrub-dominated landscapes) were explored by applying Pearson's *R* correlation. Effect significance and size was determined using a general linear model (GLM) that includes the different sources of seasonal precipitation ($Rain_{PNM}$, $Rain_{SM}$, and $Rain_{LNM}$) as covariates, landscape type (LT) as a factor, and the interaction terms between landscape type and seasonal precipitation ($LT:Rain_{PNM}$, $LT:Rain_{SM}$, and $LT:Rain_{LNM}$).

4 Results

4.1 Patterns of greenness and reference NDVI-rainfall metrics in the Core Sites

Inter- and intra-annual variations of NDVI show similar patterns of vegetation greenness for both the Black Grama and the Creosotebush Core Sites (Fig. 3a). The signal generally peaks slightly in spring (May) and strongly in summer (July-September). The lowest NDVI values

1 are observed between February and April. Summer peaks in NDVI values are, however, less
2 marked in the Creosotebush Core Site. In addition, the NDVI signal for the creosotebush-
3 dominated site generally shows an autumn (October-November) peak that is especially
4 important during particular growing cycles (2000-01, 2001-02, 2004-05, 2007-08, 2009-10).
5 Correlations between NDVI and antecedent precipitation using rainfall-accumulation lengths
6 of 1-300 days indicate that an optimal short-term cumulative rainfall period of 57 days best
7 explains the NDVI variations for the dominant herbaceous vegetation of the grassland site
8 ($ARain_{hv}$ antecedent rainfall series, with Olr_{hv} accumulation length; Fig. 3, see also
9 Supplementary Fig. 2 in the online supporting information of this study for details on the
10 annual cycles of vegetation growth). For the Creosotebush Core Site (with dominant shrub
11 vegetation and subordinate forbs and grasses), the short-term, 57-day antecedent rainfall
12 series $ARain_{hv}$ also has an important impact on the strength of the NDVI-rainfall relationship,
13 particularly for three consecutive growing cycles with strong summer precipitation (2006-07,
14 2007-08 and 2008-09, summer precipitation for the period is 40% above the long-term mean).
15 However, the NDVI-rainfall correlation in this shrub-dominated site generally peaks using a
16 much longer optimal cumulative rainfall period of nearly 145 days ($ARain_s$ series, with Olr_s
17 length).

18 **4.2 Spatial distribution of vegetation types and landscape classification**

19 PCA analysis of the NDVI-rainfall correlation coefficients (per growing cycle) for the
20 reference 57- and 145-day antecedent rainfall series (i.e. $ARain_{hv}$ and $ARain_s$ with Olr_{hv} and
21 Olr_s rainfall accumulation lengths, respectively for all MODIS pixels contained within our
22 study area) shows that PCA factor 1 (about 40% of total data variance) reflects a landscape
23 gradient that discriminates the two reference responses of vegetation greenness to antecedent
24 rainfall (Figs. 4a and 4b). The correlation between the NDVI and the short-term antecedent
25 rainfall series $ARain_{hv}$ increases to the negative side of factor 1 (particularly for growing
26 cycles 2001-02, 2002-03, 2005-06, and 2012-13), while the correlation with the 145-day
27 antecedent rainfall series ($ARain_s$) increases to the positive side of the this factor (particularly
28 for cycles 2000-01, 2002-03, 2005-06, and 2006-07, Fig. 4b). Analysis of the relationship
29 between PCA factor 1 and vegetation dominance for the ground-based set of control points
30 indicates that this landscape gradient is explained by the field distribution of dominant
31 vegetation types since the dominance of herbaceous vegetation and shrubs increases to the
32 negative and positive side of PCA factor 1, respectively (R^2 approx. 0.90, Fig. 4c).

1 Four different landscape types (GD, GT, ST and SD) are defined in the 18-km² study area as
2 determined by the spatial projection of the relationship between PCA factor 1 and field
3 dominance of herbaceous and shrub vegetation (Figs. 4c and 4d). SD, ST and GT landscapes
4 are distributed in the southwestern part of the study site, while GD landscapes are located in
5 the central and northeastern parts of the area (Figs. 4d and 4e).

6 **4.3 NDVI transformation into herbaceous and shrub ANPP components**

7 Temporal decomposition of NDVI into partial herbaceous and shrub vegetation components
8 results in very different outputs for the reference Black Grama and Creosotebush Core Sites
9 (Fig. 5a). The herbaceous component (which is derived from the relationship between NDVI
10 and the reference 57-day antecedent rainfall series, $ARain_{57}$) prevails in the grass-dominated
11 reference site, whilst the shrub component (which is function of the reference 145-day
12 antecedent rainfall series, $ARain_{145}$) comprises the leading NDVI fraction in the shrub-
13 dominated reference site.

14 The annual sums of herbaceous and shrub NDVI components for the reference Core Sites
15 show a strong linear agreement ($R^2 \geq 0.65$; $P < 0.001$) with ground-based measurements of
16 ANPP (Fig. 5b), while the remote-sensing ANPP estimations yield a root mean square error
17 of 26 g m⁻² (NRMSE 12%, Fig. 5c).

18 Spatial projection of the reference NDVI-ANPP relationships across the 18 km² study area
19 displays a contrasted distribution of mean 2000-13 ANPP for herbaceous and shrub
20 vegetation (Figs. 5d and 5e). Herbaceous ANPP is mainly distributed in the central and
21 northeastern parts of the study site, contributing to >80% total ANPP. Conversely, shrub
22 ANPP is concentrated in the southwestern edge of the study area.

23 **4.4 ANPP spatiotemporal dynamics and impact of seasonal precipitation on** 24 **herbaceous and shrub primary production**

25 Remote-sensed estimations of ANPP are significantly impacted by landscape type
26 ($F_{3, 334}=48.6$, $P < 0.01$), with grass-dominated sites supporting in general higher levels of
27 vegetation production (Fig. 6a). However, landscape-type effects are variable in time
28 (landscape type x time interaction: $F_{14, 1515}=57.2$, $P < 0.01$). Year-to-year variability of ANPP
29 is particularly large for the grass-dominated sites, which show higher levels of ANPP than the
30 transition and shrub-dominated landscapes for highly productive years (Fig. 6a). For growing

1 cycles with low primary production there are no significant ANPP differences or the
2 differences are reversed, with shrub-dominated sites showing higher production than grass-
3 dominated sites (e.g. 2003-04 cycle, Fig. 6a).

4 Analysis of the temporal evolution of shrub contribution to total ANPP along 2000-13 reflects
5 significant (although very weak) positive correlations with time for the grass- and shrub
6 transition landscapes (Fig. 6b). The same analysis at the individual pixel level, however, does
7 not show any significant correlations between shrub contribution to total ANPP and time.

8 Exploratory analysis of the influence of seasonal precipitation on remote-sensed estimations
9 of ANPP indicates different responses for herbaceous and shrub vegetation (Fig. 7).

10 Herbaceous ANPP strongly correlates with monsoonal summer precipitation for all landscape
11 types (Fig. 7a). The slope of the relationship between herbaceous ANPP and monsoonal
12 summer (June-September) precipitation decreases for the shrub-transition and shrub-
13 dominated landscapes. Conversely, shrub ANPP strongly correlates with both preceding non-
14 monsoonal (October-May) and monsoonal summer (June-September) precipitation for all
15 landscape types (Fig. 7b).

16 General linear model results confirm the exploratory observations of the relationships
17 between remote-sensed estimations of ANPP and seasonal precipitation (Table 1). Model
18 results identify both monsoonal summer precipitation ($Rain_{SM}$) and the interaction between
19 $Rain_{SM}$ and landscape type as the most important contributors (effect size, $\eta^2 > 10\%$;
20 $P < 0.001$) to the total variance comprised in ANPP data for herbaceous vegetation. Similarly,
21 non-monsoonal summer precipitation ($Rain_{PNM}$) and monsoonal summer precipitation
22 ($Rain_{SM}$) are identified as the leading contributors to shrub ANPP.

23

24 **5 Discussion**

25 **5.1 Vegetation-growth pattern and reference NDVI-rainfall metrics for** 26 **herbaceous and shrub vegetation**

27 Analysis of time series of NDVI provides important information on the dynamics of
28 vegetation growth in drylands (Peters et al., 1997; Holm et al., 2003; Weiss et al., 2004;
29 Choler et al., 2010). NDVI trends in the grass-dominated site show strong peaks centered in
30 the summer season (Fig. 3a), which agrees with both field and remote-sensed observations of

1 the dynamics of aboveground biomass for desert grasslands dominated by *Bouteloua*
2 *eriopoda* and *B. gracilis* in the area (Peters and Eve, 1995; Huenneke et al., 2002; Muldavin
3 et al., 2008; Notaro et al., 2010). For the shrub-dominated site, summer peaks in the NDVI
4 signal are smaller, and for particular years both spring and late-autumn peaks can exceed
5 summer greenness. Accordingly, the timing of plant growth for *Larrea tridentata* (which
6 dominates the reference shrubland site) has been shown to vary from year to year, since this
7 species has the ability to shift the temporal patterns of vegetation growth to take advantage of
8 changes in resource availability (Fisher et al., 1988; Reynolds et al., 1999; Weiss et al., 2004;
9 Muldavin et al., 2008).

10 The analysis of the relationships between NDVI and precipitation provide further insights on
11 plant water-use patterns and, hence, on vegetation function and structure (Pennington and
12 Collins, 2007; Veron and Paruelo, 2010; Notaro et al., 2010; Garcia et al., 2010; Forzieri et
13 al., 2011; Moreno-de las Heras et al., 2012). Temporal trends in NDVI for the reference grass-
14 and shrub-dominated SEV LTER sites are explained by antecedent (or preceding cumulative)
15 rainfall amounts, reflecting the coupling of the history of plant-available soil moisture with
16 vegetation growth (Fig. 3). Correlations between NDVI and precipitation indicate that plant
17 growth pulses for the grass-dominated site are associated with short-term antecedent rainfall
18 ($ARain_{hv}$ series; 57 days optimal length, Olr_{hv}). For the shrub-dominated landscape, vegetation
19 greenness shows a strong association with longer-term antecedent precipitation ($ARain_s$
20 series; 145 days optimal length, Olr_s), although importantly, NDVI dynamics for this site also
21 correlate with the 57-day cumulative rainfall series. Previous work on the analysis of NDVI-
22 rainfall relationships found similar variations in the length of the antecedent rainfall series
23 that best explain the dynamics of vegetation greenness, suggesting that such differences result
24 from site variations in dominant vegetation (Evans and Geerken, 2004; Prasad et al., 2007;
25 Garcia et al., 2010).

26 Given the strong relationship between time-integrated NDVI values and ground-based ANPP
27 estimations for our site (Fig. 5b), our herbaceous and shrub exploratory modeling results
28 provide a biophysical explanation for the range of variations found in the NDVI-rainfall
29 relationships (Fig. 1). The length of the cumulative precipitation series that optimizes the
30 relationship between plant biomass and antecedent rainfall (Olr) appears to be a function of
31 the characteristic water-use and plant growth pattern of dryland vegetation, that are largely
32 influenced by the plant-growth and mortality rates of vegetation (Fig. 1c). Vegetation growth

1 and water use strongly differ for herbaceous and shrub life-forms in drylands (Sparrow, 1997;
2 Ogle and Reynolds, 2004; Gilad et al., 2007; Garcia et al., 2010), in which case plant biomass
3 dynamics respond to short-term and long-term antecedent precipitation, respectively (Figs.
4 1a-b). *Olr* variations in the reference SEV LTER Core Sites may, therefore, be expressed as a
5 function of the dominant vegetation types (Fig. 3): the strong and quick responses of
6 greenness to short-term precipitation ($ARain_{hv}$) in the grass-dominated Black Grama Core Site
7 characterize herbaceous growth for the area, while the slow responses of NDVI to medium-
8 term precipitation ($ARain_s$) in the shrub-dominated Cresotebush Core Site define the
9 characteristic pattern of vegetation growth for shrubs in the ecotone. The high correlation
10 between $ARain_{hv}$ and NDVI values in the shrub-dominated Creosotebush Core Site (Fig. 3b)
11 can be explained by the growth of non-dominant herbaceous vegetation (mainly annual
12 forbs), which can be especially important during wet years (Muldavin et al., 2008; Baez et al.,
13 2012). Similarly, Moreno-de las Heras et al. (2012) in dry open-shrublands of central
14 Australia (Olr_s values about 220 days) found the emergence of secondary Olr_{hv} metrics on the
15 study of local NDVI-rainfall relationships (approx. 85 days antecedent rainfall length) caused
16 by the growth of non-dominant herbaceous vegetation. Overall, *Olr* values determined for
17 herbaceous and shrub vegetation in this work are in agreement with the range of characteristic
18 antecedent rainfall series reported in other studies to best describe green biomass dynamics
19 for arid and semi-arid grasslands (1-3 months) and woody shrublands (4-8 months) (Evans
20 and Geerken, 2004; Munkhtsetseg et al., 2007; Garcia et al., 2010; Moreno-de las Heras et al.,
21 2012).

22 **5.2 Spatial distribution and net primary production of herbaceous vegetation** 23 **and shrubs**

24 Our results indicate that the relationship between temporal series of remotely sensed NDVI
25 and antecedent precipitation is highly sensitive to spatial differences in dominant vegetation
26 (Fig. 4). The main PCA factor (explaining about 40% variance in data) extracted using the
27 annual NDVI responses (i.e. the Pearson's *R* coefficients) to the reference 57- and 145-day
28 characteristic antecedent rainfall series ($ARain_{hv}$ and $ARain_s$ series, respectively) accurately
29 discriminates the behavior of herbaceous and shrub vegetation for the 18 km² study area
30 (Figs. 4b-c), hence providing a robust approach for classifying landscapes as a function of the
31 dominance of vegetation types using coarse-grained remotely sensed data (Fig. 4d). This
32 parsimonious approach offers a practical alternative to other more complex remote-sensing

1 methodologies for the analysis of the spatial distribution of vegetation types in mixed
2 systems, such as Spectral Mixture Analysis (SMA, Smith et al., 1990), which may be difficult
3 to apply in this Chihuahuan case study since both the mixed nature and fine-grained
4 distribution of vegetation in the area (patches of grass and shrubs are typically $<1 \text{ m}^2$ and 0.5-
5 5 m^2 , respectively; Turnbull et al. 2010b) can impose serious drawbacks on the detection of
6 reference spectral signatures for pure herbaceous and shrub vegetation using coarse-grained
7 MODIS data. Implementing SMA-based approaches for the analysis of vegetation distribution
8 and landscape classification in drylands using medium- and coarse-grained data is very
9 challenging since it requires significant amounts of ancillary data (e.g. laboratory-based or
10 field multi-date spectra for vegetation types) to solve data uncertainties generated by surface
11 heterogeneity, which is often not feasible (Somers et al. 2011).

12 The relationships of vegetation greenness to $ARain_{hv}$ and $ARain_s$ also provide criteria for
13 decomposing and transforming the NDVI signal into structural components of primary
14 production for this study. Lu et al. (2003) applied seasonal trend decomposition to partition
15 NDVI into (cyclic) herbaceous and (trend) woody vegetation in Australia. They assumed a
16 long-term weak phenological wave and a strong annual response for determining the shrub
17 and herbaceous components of vegetation, respectively. Our approach relies on the use of
18 differences in biophysical properties of herbaceous and shrub vegetation related to the
19 coupling between vegetation growth and precipitation for decomposing the NDVI signal,
20 rather than apparent differences in the seasonality of vegetation greenness alone. As expected,
21 signal decomposition outcomes indicate that the herbaceous component of the NDVI leads the
22 temporal trends for the grass-dominated reference Black Grama Core Site, while the shrub
23 component largely dominates the NDVI signal for the Creosotebush Core Site (Fig. 5a).

24 Although affected by data dispersion, the annual sums of decomposed NDVI strongly agree
25 with field estimations of ANPP for herbaceous and shrub vegetation ($R^2 \geq 0.65$, Fig. 5b),
26 resulting in a small root mean square error for our remote-sensing ANPP estimates (26 g m^{-2} ,
27 NRMSE 12%, Fig 5c) that is within the lower limit of reported errors by other NDVI
28 decomposition studies (for example, Roderick et al., 1999; DeFries et al., 2000, Hansen et al.,
29 2002; Lu et al., 2003; with NRMSE ranging 10-17%). Other dryland studies have found
30 important levels of data dispersion when relating fine-grained field ANPP to coarse-scale
31 NDVI values (Lu et al., 2003; Holm et al., 2003; Pennington and Collins, 2007; Veron and
32 Paruelo, 2010). Major sources of data dispersion for this study are most likely associated with

1 the high spatial variability of ANPP in the analyzed systems. For instance, field estimations
2 have shown that ANPP for both grass- and shrub-dominated Chihuahuan landscapes are
3 affected by important levels of spatial variability, primarily due to the patchiness of
4 vegetation cover (Huenneke et al., 2002; Muldavin et al., 2008).

5 **5.3 Spatiotemporal dynamics of ANPP and impact of seasonal precipitation** 6 **on herbaceous and shrub primary production**

7 Cross-scale interactions between vegetation composition, individual plant characteristics and
8 climatic drivers (e.g. variations in precipitation amount and seasonality) have an important
9 role on determining primary production patterns in arid and semi-arid ecosystems (Peters,
10 2002; Snyder and Tartowsky, 2006; Pennington and Collins, 2007; Notaro et al., 2010; Baez
11 et al., 2013). Analysis of the spatiotemporal dynamics of ANPP in our ecotone indicates that
12 grass-dominated sites, although very importantly affected by year-to-year variability,
13 generally support higher primary production than transition and shrub-dominated landscapes,
14 particularly for wet years with high ANPP levels (Fig. 6a). This result is consistent with other
15 shrub-encroachment studies which have found associations between shrub proliferation and
16 ANPP reductions in dry American grasslands (Huenneke et al., 2002; Knapp et al., 2008).

17 Our results suggest that primary production is differently controlled by seasonal precipitation
18 for herbaceous and shrub vegetation across the 18-km² Chihuahuan Desert ecotone (Fig 7,
19 Table 1). Monsoonal summer precipitation (June-September) controls ANPP for herbaceous
20 vegetation (Fig. 7a), while ANPP for shrubs is better explained by the preceding year's non-
21 monsoonal (October-May) plus the summer monsoonal precipitation in the present year (Fig
22 7b). Accordingly, field observations of ANPP for Chihuahuan landscapes found that
23 grassland primary production is particularly coupled with monsoonal rainfall, while desert
24 shrublands appear to be less dependent on summer precipitation (Fisher et al., 1988; Reynolds
25 et al., 1999; Huenneke et al., 2002; Muldavin et al., 2008; Throop et al., 2012).

26 Differences in the distribution of rainfall types, soil-moisture dynamics, and rooting habits of
27 dominant plant species may explain the variable impact of seasonal precipitation on
28 herbaceous and shrub ANPP for the studied Chihuahuan landscapes. Monsoonal summer
29 precipitation (July-September, approx. 60% annual precipitation) generally takes place in the
30 form of high-intensity thunderstorms that infiltrate shallow soil depths (top 15-35 cm)
31 (Snyder and Tartowsky, 2006). Summer soil-water resources for plant production are

1 ephemeral and strongly affected by evapotranspiration, which typically reduces soil moisture
2 to pre-storm background levels in 4-7 days after rainfall (Turnbull et al., 2010a). C₄ grasses
3 (*Bouteloua eriopoda* and *B. gracilis*), which dominate herbaceous vegetation in the analyzed
4 ecotone, concentrate active roots in the top 30 cm of the soil and intensively exploit
5 ephemeral summer soil moisture for plant growth (Peters, 2002; Muldavin et al., 2008).
6 Preferential spatial redistribution of runoff to grass patches following summer storms further
7 enhances plant production for black and blue grama (Wainwright et al., 2000; Pockman and
8 Small, 2010; Turnbull et al., 2010b).

9 Non-monsoonal precipitation (about 40% annual precipitation, primarily from November to
10 February) typically falls in the form of long-duration low-intensity frontal rainfall that often
11 percolates to deep soil layers (Snyder and Tartowsky, 2006). *Larrea tridentata*, the dominant
12 C₃ shrub in the studied ecotone, has a bimodal rooting behavior that facilitates the use of both
13 shallow and deep soil moisture for plant production (Fisher et al., 1988; Reynolds et al., 1999;
14 Ogle and Reynolds, 2004). Deep creosotebush roots (70-150 cm depth) may acquire winter-
15 derived soil-water resources that are unavailable to grass species, while active roots near the
16 surface (20-40 cm depth) may serve to access summer-derived shallow soil moisture for plant
17 growth (Gibbens and Lenz, 2001). The observed reduction in summer rain-use efficiency of
18 herbaceous vegetation for the shrub-transition and shrub-dominated landscapes (i.e. variations
19 on the slope of the relationship between herbaceous ANPP and summer precipitation, Fig. 7a)
20 suggests competitive effects of creosotebush for the use of shallow water sources, probably
21 associated to the large spatial extent of near-surface active roots (the radial spread of which
22 typically ranges between 2-6 m, Gibbens and Lenz, 2001). Alternative, landscape changes
23 induced by shrub encroachment (i.e. increased runoff and erosion) may reduce the ability of
24 grass patches to capitalize on horizontal redistribution of runoff for plant growth after summer
25 storms (Wainwright et al., 2000; Turnbull et al., 2012; Stewart et al. 2014).

26 Conceptual and mechanistic models of vegetation change suggest that vegetation composition
27 in arid and semi-arid landscapes is likely to be highly sensitive to climate change, and point at
28 variations in the amount and distribution of precipitation as a major driver of shrub
29 encroachment into desert grasslands (Peters, 2002; Gao and Reynolds, 2003; Snyder and
30 Tartowsky, 2006). Overall our results agree with those findings and suggest that changes in
31 the amount and temporal pattern of precipitation comprising reductions in monsoonal summer
32 rainfall and/or increases in winter precipitation may enhance the encroachment of

1 creosotebush into desert grasslands dominated by black and blue grama. Analysis of long-
2 term rainfall series indicates that winter precipitation has increased during the past century in
3 the northern Chihuahuan Desert, particularly since 1950, probably associated with the more
4 frequent occurrence of ENSO events for that period (Dahm and Moore, 1994; Wainwright,
5 2006). This pattern of precipitation change may be responsible, at least in part, of past
6 increase in woody shrub abundance over desert grasslands in the American Southwest (Brown
7 et al., 1997; Snyder and Tartowsky, 2006; Webb et al., 2003). Our results suggest that shrub
8 encroachment has not been particularly active in the studied ecotone for 2000-13 (Fig. 6b).
9 Accordingly, Allen et al. (2008) in a recent study on creosotebush plant architecture and age
10 structure indicated that the most important pulses of shrub encroachment for this area took
11 place between 1950 and 1970. Precise estimation of shrub cover applying segmentation
12 methods in time series of high-resolution imagery could help to accurately determine the
13 intensity of the shrub-encroachment phenomenon under the present variability in precipitation
14 for our grassland-shrubland ecotone.

15 Climate-change projections for the area suggest a general picture of increased aridity in the
16 next 100 years, with increased evaporation due to higher summer temperatures, and increased
17 drought frequency (Christensen and Konikicharla, 2013). The capacity of *L. tridentata* to
18 switch between different soil-water sources (i.e. summer-derived ephemeral shallow soil
19 moisture and more stable deep soil-water reserves derived from winter rainfall) and adapt the
20 timing of vegetation growth to take advantage of changes in resource availability make this C₃
21 shrub less susceptible to predicted increases in aridity than C₄ grasses that are strongly
22 dependent on summer precipitation (Reynolds et al., 1999; Throop et al., 2012; Baez et al.,
23 2013). Current increases in atmospheric CO₂ concentrations may also contribute to reduce the
24 competitiveness of C₄ grasses for the use of soil-water resources against C₃ desert shrubs
25 (Polley et al., 2002). Remaining desert grasslands in the American Southwest may, therefore,
26 be increasingly susceptible to shrub encroachment under the present context of changes in
27 climate and human activities.

28

29 **6 Conclusions**

30 In this study we applied a new analytical methodology for the study of the organization and
31 dynamics of vegetation at a grassland-shrubland Chihuahuan ecotone with variable abundance
32 of grasses (primarily *Bouteloua eriopoda* and *B. gracilis*) and shrubs (mainly *Larrea*

1 *tridentata*), based on the exploration of the relationship between time series of remote-sensed
2 vegetation greenness (NDVI) and precipitation. Our results indicate that the characteristics of
3 the NDVI-rainfall relationships are highly dependent on differences in patterns of water use
4 and plant growth of vegetation types. In fact, NDVI-rainfall relationships show a high
5 sensitivity to spatial variations on dominant vegetation types across the grassland-shrubland
6 ecotone, and provide ready biophysically based criteria to study the spatial distribution and
7 dynamics of net primary production (NPP) for herbaceous and shrub vegetation. The analysis
8 of the relationship between NDVI and precipitation offers, therefore, a powerful methodology
9 for the study of broad-scale vegetation shifts comprising large changes in the dominance of
10 vegetation types in drylands using coarse-grained remotely sensed data, and could be used to
11 target areas for more detailed analysis and/or the application of mitigation measures.

12 Analysis of remote-sensed NPP dynamics at the grassland-shrubland ecotone reflects a
13 variable performance of dominant vegetation types. Herbaceous production is synchronized
14 with monsoonal summer rainfall, while shrub NPP shows a flexible response to both summer
15 and winter precipitation. Overall our results suggest that changes in the amount and temporal
16 pattern of precipitation (i.e. reductions in summer precipitation and/or increases in winter
17 rainfall) may intensify the shrub-encroachment process in the studied desert grasslands of the
18 American Southwest, particularly in the face of predicted general increases in aridity and
19 drought frequency for the area.

20

21 **Acknowledgements**

22 We would like to thank the Sevilleta LTER team, and particularly Scott L. Collins, John
23 Mulhouse and Amaris L. Swann, for logistic support and for granting access to the SEV
24 LTER Five Points NPP and rainfall datasets. We also thank Patricia M. Saco for field
25 assistance. Fieldwork at the Sevilleta National Wildlife Refuge for this study was carried out
26 under permit 22522-14-32, granted by the US Fish and Wildlife Service. An earlier version of
27 this paper benefited from the helpful comments of two anonymous referees. This work is
28 supported by a FP7 Marie Curie IEF fellowship funded by the European Commission (PIEF-
29 GA-2012-329298, VEGDESERT). Significant funding for collection of the SEV LTER data
30 was provided by the National Science foundation Long Term Ecological Research program
31 (NSF grant numbers BSR 88-11906, DEB 0080529, and DEB 0217774).

32

1 **References**

- 2 Al-Bakri, J. T., and Suleiman, A. S.: NDVI response to rainfall in different ecological zones
3 in Jordan, *Int. J. Remote Sens.*, 10, 3897-3912, 2004.
- 4 Allen, A. P., Pockman, W. T., Restrepo, C., and Milne, B. T.: Allometry, growth and
5 population regulation of the desert shrub *Larrea tridentata*, *Funct. Ecol.*, 22, 197-204, 2008.
- 6 Anderson, G. L., Hanson, J. D., and Haas., R. H.: Evaluating Landsat Thematic Mapper derived
7 vegetation indices for estimating above-ground biomass on semiarid rangelands, *Remote Sens.*
8 *Environ.*, 45, 165-175, 1993.
- 9 Baez, S., Collins, S. C., Pockman, W. T., Johnson, J. E., and Small, E. E.: Effects of
10 experimental rainfall manipulations on Chihuahuan Desert grassland and shrubland plant
11 communities, *Oecologia*, 172, 1117-1127, 2013.
- 12 Brown, J. H., Valone, T. J., and Curtin, C. G.: Reorganization of an arid ecosystem in response
13 to recent climate change, *P. Natl. Acad. Sci. USA.*, 94, 9729-9733, 1997.
- 14 Buffington, L. C., and Herbel, C. H.: Vegetational changes on a semidesert grassland range
15 from 1858 to 1963, *Ecol. Monogr.*, 35, 139-164, 1965.
- 16 Carlson, T. N., and Ripley, D. A.: On the relation between NDVI, fractional cover, and leaf
17 area index, *Remote Sens. Environ.*, 62, 241-252, 1997.
- 18 Choler, P., Sea, W., Briggs, P., Raupach, M., and Leuning, R.: A simple ecohydrological
19 model captures essentials of seasonal leaf dynamics in semiarid tropical grasslands,
20 *Biogeosciences*, 7, 907-920, 2010.
- 21 Christensen, J. H, and Konikicharla, K. K.: Climate phenomena and their relevance for future
22 regional climate change, in: *Climate Change 2013: The Physical Science Basis, Contribution of*
23 *Working Group I to the Fifth Assessment Report of the Intergovernmental Panel on Climate*
24 *Change*, edited by: Stoker, T. F., Qin, D., Platter, G. K., Tignor, M., Allen, S. K., Boschung, J.,
25 Navels, A., Xia, Y., Bex, V., and Midgley, P. M., Cambridge University Press, Cambridge, UK,
26 1217-1308, 2013.
- 27 Collins, S. L., Belnap, J., Grimm, N. B., Rudgers, J. A., Dahm, C. N., D'Odorico, P., Litvak,
28 M., Natvig, D. O., Peters, D. C., Pockman, W. T., Sinsabaugh, R. L., and Wolf, B. O.: A
29 multiple, hierarchical model of pulse dynamics in arid-land ecosystems, *Annu. Rev. Ecol. Evol.*
30 *Syst.*, 45, 397-419, 2014.

- 1 Dahm, C. N., and Moore, D. I.: The El Niño/Southern Oscillation phenomenon and the
2 Sevilleta Long-Term Ecological Research site, in: El Niño and Long-Term Ecological Research
3 (LTER) Sites, edited by: Greenland, D., LTER Network Office, University of Washington,
4 Seattle, USA, 12-20, 1994.
- 5 DeFries, R. S., Hansen, M. C., and Townshend, J. R.G.: Global continuous fields of vegetation
6 characteristics: a linear mixture model applied to multiyear 8 km AVHRR data, *Int. J. Remote*
7 *Sens.*, 21, 1389-1414, 2000.
- 8 D'Odorico, P., Okin, G. S., and Bestelmeyer, B. T.: A synthetic review of feedbacks and
9 drivers of shrub encroachment in arid grasslands, *Ecohydrology*, 5, 520-530, 2012.
- 10 Evans, J., and Geerken, R.: Discrimination between climate and human-induced dryland
11 degradation, *J. Arid Environ.*, 57, 535-554, 2004.
- 12 Fisher, F. M., Zak, J. C., Cunningham, G. L., and Whitford, W. G.: Water and nitrogen effects
13 on growth and allocation patterns of creosotebush in the northern Chihuahuan Desert, *J. Range*
14 *Manage.*, 41, 387-391, 1988.
- 15 Forzieri, G., Castelli, F., and Vivoni, E. R.: Vegetation dynamics within the North American
16 Monsoon Region, *J. Climate*, 24, 1763-83, 2011.
- 17 Gao, Q., and Reynolds, J. F.: Historical shrub-grass transitions in the northern Chihuahuan
18 Desert: Modeling the effects of shifting rainfall seasonality and event size over a landscape,
19 *Global Change Biol.*, 9, 1-19, 2003.
- 20 Garcia, M., Litago, J., Palacios-Orueta, A., Pinzon, J. E., and Ustin, S. L.: Short-term
21 propagation of rainfall perturbations on terrestrial ecosystems in central California, *Appl. Veg.*
22 *Sci.*, 13, 146-162, 2010.
- 23 Gibbens, R. P., and Lenz, J. M.: Root systems of some Chihuahuan Desert plants, *J. Arid*
24 *Environ.*, 49, 221-263, 2001.
- 25 Gilad, E., Shachak, M., and Meron, E.: Dynamics and spatial organization of plant
26 communities in water-limited systems, *Theor. Popul. Biol.*, 72, 214-230, 2007.
- 27 Girden, E. R.: ANOVA: repeated measures, SAGE University Paper Series 7-84, SAGE
28 Publications, Newbury Park, USA, 1992.

- 1 Godin-Alvarez, H., Herrick, J. E., Mattocks, M., Toledo, D., and Van Zee, J.: Comparison of
2 three vegetation monitoring methods: their relative utility for ecological assessment and
3 monitoring, *Ecol. Indic.*, 9, 1001-1008, 2009.
- 4 Gosz, J. R.: Ecological functions in a biome transition zone: translating local responses to
5 broad-scale dynamics, in: *Landscape Boundaries: Consequences for Biotic Diversity and
6 Ecological Flows*, edited by: Hansen, A. J., and di Castri, A. J., Springer, New York, USA, 56-
7 75, 1992.
- 8 Hansen, M. C., DeFries, R. S., Townshend, J. R. G., Sohlberg, R., Dimiceli, C., and Carroll,
9 M.: Towards an operational MODIS continuous field of percent tree cover algorithm: examples
10 using AVHRR and MODIS data, *Remote Sens. Environ.*, 83, 303-319, 2002.
- 11 Holm, A. McR., Cridland, S. W., and Roderick, M. L.: The use of time-integrated NOAA
12 NDVI data and rainfall to assess landscape degradation in the arid and shrubland of Western
13 Australia, *Remote Sens. Environ.*, 85, 145-158, 2003.
- 14 Hueneke, L. F., Anderson, J. P., Remmenga, M., and Schlesinger, W. H.: Desertification alters
15 patterns of aboveground net primary production in Chihuahuan ecosystems, *Global Change
16 Biol.*, 8, 247-264, 2002.
- 17 Huete, A., Jackson, R. D., and Post, D. F.: Spectral response of a plant canopy with different
18 soil backgrounds, *Remote Sens. Environ.*, 17, 37-53, 1985.
- 19 Huete, A., Didan, K., Miura, T., Rodriguez, E. P., Gao, X., and Ferreira, L. G.: Overview of the
20 radiometric and biophysical performance of the MODIS vegetation indices, *Remote Sens.
21 Environ.*, 83,195-213, 2002.
- 22 Lu, H., Raupach, M. R., McVicar, T. R., and Barret, D. J.: Decomposition of vegetation cover
23 into woody and herbaceous components using AVHRR NDVI time series, *Remote Sens.
24 Environ.*, 86, 1-16, 2003.
- 25 Millennium Ecosystem Assessment: Ecosystems and Human Well-being: Biodiversity
26 Synthesis, World Resources Institute, Washington, DC, USA, 2005.
- 27 Montandon, L. M., and Small, E. E.: The impact of soil reflectance on the quantification of the
28 green vegetation fraction from NDVI, *Remote Sens. Environ.*, 112, 1835-1845, 2008.

- 1 Moreno-de las Heras, M., Saco, P. M., Willgoose, G. R., and Tongway, D. J.: Variations in
2 hydrological connectivity of Australian semiarid landscapes indicate abrupt changes in rainfall-
3 use efficiency of vegetation, *J. Geophys. Res.*, 117, G03009, doi:10.1029/2011JG001839, 2012.
- 4 Mueller E. N., Wainwright, J., and Parsons, A. J.: The stability of vegetation boundaries and
5 the propagation of desertification in the American Southwest: A modelling approach, *Ecol.*
6 *Model.*, 208, 91-101, 2007.
- 7 Muldavin, E. H., Moore, D. I., Collins, S. L., Wetherill, K. R., and Lightfoot, D. C.:
8 Aboveground net primary production dynamics in a northern Chihuahuan Desert ecosystem,
9 *Oecologia*, 155, 123-132, 2008.
- 10 Munkhtsetseg, E., Kimura, R., Wand, J., and Shinoda, M.: Pasture yield response to
11 precipitation and high temperature in Mongolia, *J. Arid Environ.*, 70, 1552-1563, 2007.
- 12 Notaro, M., Liu, Z., Gallimore, R. G., Williams, J. W., Gutzler, D. S., and Collins, S.: Complex
13 seasonal cycle of ecohydrology in the Southwest United States, *J. Geophys. Res.*, 115, G04034,
14 doi: 10.1029/2010JG001382, 2010.
- 15 Ogle, K., and Reynolds, J. F.: Plant responses to precipitation in desert ecosystems: integrating
16 functional types, pulses, thresholds and delays, *Oecologia*, 141, 282-294, 2004.
- 17 Okin, G. S., and Roberts, D.A.: Remote sensing in arid environments: challenges and
18 opportunities, in: *Manual of Remote Sensing Vol 4: Remote Sensing for Natural Resource*
19 *Management and Environmental Monitoring*, edited by: Ustin, S., John Willey and Sons, New
20 York, USA, 111-146, 2004.
- 21 Okin, G. S., Roberts, D. A., Murray, B., and Okin, W. J.: Practical limits on hyperspectral
22 vegetation discrimination in arid and semiarid environments, *Remote Sens. Environ.*, 77, 212-
23 225, 2001.
- 24 Okin, G. S., Parsons, A. J., Wainwright, J., Herrick, J. E., Bestelmeyer, B. T., Peters, D. C., and
25 Fredrickson, E. L.: Do changes in connectivity explain desertification? *BioScience*, 59, 237-
26 244, 2009.
- 27 Pennington, D. D., and Collins, S. L.: Response of an aridland ecosystem to interannual climate
28 variability and prolonged drought, *Landscape Ecology*, 22, 897-910, 2007.
- 29 Peters, D. P. C.: Plant species dominance at a grassland-shrubland ecotone: and individual-
30 based gap dynamics model of herbaceous and woody species, *Ecol. Model.*, 152, 5-32, 2002.

- 1 Peters, A. J., and Eve, M. D.: Satellite monitoring of desert plant community response to
2 moisture availability, *Environ. Monit. Assess.*, 37, 273-287, 1995.
- 3 Peters, A. J., Eve, M. D., Holt, E. H., and Whitford, W. G.: Analysis of desert plant community
4 growth patterns with high temporal resolution satellite spectra, *J. Appl. Ecol*, 34, 418-432,
5 1997.
- 6 Petrie, M. D., Collins, S. L., Gutzler, D. S., and Moore, D. M.: Regional trends and local
7 variability in monsoon precipitation in the northern Chihuahuan desert, USA, *J. Arid Environ*,
8 103, 63-70, 2014.
- 9 Pockman, W. T., and Small, E. E.: The influence of spatial patterns of soil moisture on the
10 grass and shrub responses to a summer rainstorm in a Chihuahuan desert ecotone, *Ecosystems*,
11 13, 511-525, 2010.
- 12 Polley, H. W., Johnson, H. B., and Tischler, C. R.: Woody invasion of grasslands: evidence that
13 CO₂ enrichment indirectly promotes establishment of *Prosopis glandulosa*, *Plant Ecol.*, 164,
14 85-94, 2002.
- 15 Prasad, V. K., Badarinath, K. V. S., and Eaturu, A.: Spatial patterns of vegetation phenology
16 metrics and related climatic controls of eight contrasting forest types in India-analysis from
17 remote sensing datasets, *Theor Appl Climatol*, 89, 95-107, 2007.
- 18 Ravi, S, Breshears, D. D., Huxman, T. E., and D'Odorico, P.: Land degradation in drylands:
19 Interactions among hydrologic-aeolian processes and vegetation dynamics, *Geomorphology*,
20 116, 236-245, 2010.
- 21 Reynolds, J. F., Virginia, R. A., Kemp, P. R., de Soyza, A. G., and Tremmel, D. C.: Impact of
22 drought on desert shrubs: effects of seasonality and degree of resource island development,
23 *Ecol. Monogr.*, 69, 69-106, 1999.
- 24 Reynolds, J. F., Kemp, P. R., Ogle, K., and Fernandez, R. J.: Modifying the 'pulse-reserve'
25 paradigm for deserts of North America: precipitation pulses, soil water, and plant responses,
26 *Oecologia*, 141, 194-210, 2004.
- 27 Rietkerk, M., Boerlijst, M. C., Van Langevelde, F., HilleRisLambers, R., Van de Koppel, J.,
28 Kumar, L., Prins, H. H. T., and de Roos, A. M.: Self-organization of vegetation in arid
29 ecosystems, *Am. Nat.*, 160, 524-530, 2002.

- 1 Roderick, M. L., Noble, I. R., and Cridland, S. W.: Estimating woody and herbaceous cover
2 from time series satellite observations, *Global Ecol. Biogeogr.*, 8, 501-508, 1999.
- 3 Saco, P. M., and Moreno-de las Heras, M.: Ecogeomorphic coevolution of semiarid hillslopes:
4 emergence of banded and striped vegetation patterns through interaction of biotic and abiotic
5 processes, *Water Resour. Res.*, 49, 115-126, 2013.
- 6 Schwinning, S. and Sala, O.E.: Hierarchy of responses to resource pulses in arid and semi-arid
7 ecosystems, *Oecologia*, 141, 211-220, 2004.
- 8 Schlesinger, W. H., Reynolds, J. F., Cunningham, G. L., Hueneke, L. F., Jarrell, W. M.,
9 Virginia, R. A., and Whitford, W. G.: Biological feedbacks in global desertification, *Science*,
10 247, 1043-1048, 1990.
- 11 Smith, M. O., Ustin, S. L., Adams, J. B., and Gillespie, A. R.: Vegetation in deserts: I. a
12 regional measure of abundance from multispectral images, *Remote Sens. Environ.*, 31, 1-26,
13 1990.
- 14 Snyder, K. A., and Tartowsky, S. L.: Multi-scale temporal variation in water availability:
15 Implications for vegetation dynamics in arid and semi-arid ecosystems, *J. Arid Environ*, 65,
16 219-234, 2006.
- 17 Soil Survey Staff: Keys to Soil Taxonomy, 11th Ed., USDA Natural Resources Conservation
18 Service, Washington, USA, 2010.
- 19 Somers, B., Asner, G. P., Tits, L., and Coppin, P.: Endmember variability in Spectral Mixture
20 Analysis: A review, *Remote Sens. Environ.*, 115,1603-1616, 2011.
- 21 Sparrow, A. D., Friedel, M. H., Stafford-Smith, D. M.: A landscape-scale model of shrub and
22 herbage dynamics in Central Australia, validated by satellite data, *Ecol. Model.*, 97, 197-213,
23 1997.
- 24 Stewart, J., Parsons, A. J., Wainwright, J., Okin, G. S., Bestelmeyer, B. T., Fredrickson, E. L.,
25 and Schlesinger, W. H.: Modelling emergent patterns of dynamic desert ecosystems, *Ecol.*
26 *Monogr.*, 84, 373-410, 2014.
- 27 Throop, H. L., Reichman, L. G., and Archer, S. R.: Response of dominant grass and shrub
28 species to water manipulation: an ecophysiological basis for shrub invasion in a Chihuahuan
29 Desert grassland, *Oecologia*, 169, 373-383, 2012.

1 Turnbull, L., Brazier, R. E., Wainwright, J., Dixon, L., and Bol, R.: Use of carbon isotope
2 analysis to understand semi-arid erosion dynamics and long-term semi-arid degradation, *Rapid*
3 *Commun. Mass Sp.*, 22, 1697-1702, 2008.

4 Turnbull, L., Wainwright, J., and Brazier, R. E.: Changes in hydrology and erosion over a
5 transition from grassland to shrubland, *Hydrol. Process.*, 24, 393-414, 2010a.

6 Turnbull, L., Wainwright, J., Brazier, R. E., and Bol, R.: Biotic and abiotic changes in
7 ecosystem structure over a shrub-encroachment gradient in the southwestern USA, *Ecosystems*,
8 13, 1239-1255, 2010b.

9 Turnbull, L., Wainwright, J. and Ravi, S.: Vegetation change in the southwestern USA: patterns
10 and processes, in: *Patterns of Land Degradation in Drylands, Understanding Self-Organised*
11 *Ecogeomorphic Systems*, edited by: Mueller, E. N., Wainwright, J., Parsons, A. J., and
12 Turnbull, L., Springer, New York, USA, 289-313, 2014.

13 Turnbull, L., Wilcox, B. P. , Belnap, J., Ravi, S., D'Odorico, P., Childers, D. L., Gwenz, W.,
14 Okin, G. S., Wainwright, J., Caylor, K. K., and Sankey T.: Understanding the role of
15 ecohydrological feedbacks in ecosystem state change in drylands, *Ecohydrology*, 5, 174-183,
16 2012.

17 Turnbull, L., Parsons, A. J., Wainwright, J., and Anderson, J. P.: Runoff responses to long-term
18 rainfall variability in a shrub-dominated catchment, *J. Arid Environ*, 91, 88-94, 2013.

19 van Auken, O. W.: Shrub invasions of North American semiarid grasslands, *Annu. Rev. Ecol.*
20 *Syst.*, 12, 352-356, 2000.

21 Veron, S. R., and Paruelo, V.: Desertification alters the response of vegetation to changes in
22 precipitation, *J. App. Ecol.*, 47, 1233-1241, 2010.

23 Wainwright, J.: Climate and climatological variations in the Jornada Range and neighboring
24 areas of the US South West, *Advances in Environmental Monitoring and Modelling*, 1, 39-110,
25 2005.

26 Wainwright, J., Parsons, A. J., and Abrahams, A. D.: Plot-scale studies of vegetation, overland
27 flow and erosion interactions: case studies from Arizona and New Mexico, *Hydrol. Process.*,
28 14, 2921-2943, 2000.

- 1 Webb, R. H., Turner, R. M., Bowers, J. E., and Hastings, J. R.: The Changing Mile Revisited.
- 2 An Ecological Study of Vegetation Change with Time in the Lower Mile of an Arid and
- 3 Semiarid Region, University of Arizona, Tucson, USA, 2003.
- 4 Weiss, J. L., Gutzler, D. S., Coonrod, J. E. A., and Dahm, C. N.: Long-term vegetation
- 5 monitoring with NDVI in a diverse semi-arid setting, central New Mexico, USA, *J. Arid*
- 6 *Environ.*, 58, 249-272, 2004.
- 7

1 **Table 1.** Main effects and interactions of seasonal precipitation (preceding non-monsoonal
2 rainfall, October-May; monsoonal summer rainfall, June-September; late non-monsoonal
3 rainfall, October-March) and landscape type (4 levels: grass-dominated, grass-transition,
4 shrub-transition, and shrub-dominated landscapes) on remote-sensing estimated annual (per
5 growing cycle, April-March) net primary production for herbaceous vegetation and shrubs.

| | <i>F</i> | df | <i>P</i> | η^2 (%) |
|---|----------|----|----------|--------------|
| Herbaceous vegetation ANPP_{r.sensing} | | | | |
| Rain _{PNM} (Oct-May) | 194.2 | 1 | 0.000 | 4.2 |
| Rain _{SM} (June-Sept.) | 1483.4 | 1 | 0.000 | 25.4 |
| Rain _{LNM} (Oct.-March) | 129.3 | 1 | 0.000 | 2.0 |
| LT | 35.9 | 3 | 0.000 | 2.3 |
| LT:Rain _{PNM} (Oct-May) | 122.4 | 3 | 0.000 | 7.8 |
| LT:Rain _{SM} (June-Sept.) | 282.4 | 3 | 0.000 | 16.2 |
| LT:Rain _{LNM} (Oct.-March) | 1.1 | 3 | 0.326 | 0.0 |
| Shrubs ANPP_{r.sensing} | | | | |
| Rain _{PNM} (Oct-May) | 1661.2 | 1 | 0.000 | 27.7 |
| Rain _{SM} (June-Sept.) | 1720.8 | 1 | 0.000 | 28.4 |
| Rain _{LNM} (Oct.-March) | 7.1 | 1 | 0.010 | 0.1 |
| LT | 2.9 | 3 | 0.030 | 0.2 |
| LT:Rain _{PNM} (Oct-May) | 6.6 | 3 | 0.000 | 0.4 |
| LT:Rain _{SM} (June-Sept.) | 46.2 | 3 | 0.000 | 3.0 |
| LT:Rain _{LNM} (Oct.-March) | 31.9 | 3 | 0.000 | 2.1 |

6 Abbreviations: ANPP_{r.sensing}, remote-sensed annual net primary production; Rain_{PNM} (Oct-May),
7 preceding non-monsoonal rainfall; Rain_{SM} (June-Sept.), monsoonal summer rainfall; Rain_{LNM} (Oct.-
8 March), late non-monsoonal rainfall; LT, landscape type; ':', interaction terms; η^2 , eta-squared
9 (effect size).

10 Notes: η^2 values in bold are > 10% (effects that contribute in more than 10% to the total
11 variance comprised in ANPP_{r.sensing}).

12

1 **Fig. 1.** Simulated dryland biomass-rainfall relationships for herbaceous and shrub vegetation:
2 (a) modelled biomass dynamics for an herbaceous (green) and a shrub (red) species, (b)
3 strength of the biomass-precipitation relationship (Pearson's R correlation) using different
4 lengths of rainfall accumulation for the simulated herbaceous and shrub species (values above
5 the dotted grey line are significant at $P < 0.05$), (c) optimal rainfall accumulation length (Olr)
6 as a function of the plant-growth and mortality rates. $ARain_{hv}$ and $ARain_s$ lines in panel (a)
7 represent the antecedent rainfall series that best correlate with the simulated series of
8 herbaceous and shrub biomass, respectively (i.e. time series of precedent rainfall with rainfall
9 accumulation lengths Olr_{hv} for herbaceous vegetation and Olr_s for shrubs). The green and red
10 dots in panel (c) indicate optimal rainfall accumulation lengths obtained for the simulated
11 herbaceous (Olr_{hv} , 52 days) and shrub (Olr_s , 104 days) species, respectively. The (grey)
12 "vegetation extinction" area in panel (c) reflects combined values of plant-growth and
13 mortality rates that do not support long-term vegetation dynamics for the simulated rainfall
14 conditions.

15

16 **Fig. 2.** Study area: (a) location of the Sevilleta National Wildlife Refuge (SNWR) and
17 distribution of major New Mexico biomes, (b) regional location of the study area (McKenzie
18 Flats, SNWR), (c) detailed location of the study site (18-km² area) and general view of the
19 reference SEV LTER Black Grama (right) and Creosotebush (left) Core Sites. Map (a)
20 follows the Sevilleta LTER classification of New Mexico biomes (Sevilleta LTER,
21 <http://sev.lternet.edu/content/new-mexico-biomes-created-sevlter>). Source for background
22 image in panels (b) and (c): 2009 National Aerial Imagery Program (USDA Farm Service
23 Agency).

24

25 **Fig. 3.** Reference NDVI-rainfall relationships at the SEV LTER Black Grama and
26 Creosotebush Core Sites: (a) 2000-13 MODIS NDVI time series for the Core Sites, (b)
27 strength of the NDVI-rainfall relationship (Pearson's R correlation) for the Core Sites using
28 different lengths of rainfall accumulation (maximum correlations, R_{max} , for the annual cycles
29 of vegetation growth are shown together with the 2000-13 mean trend; detailed correlograms
30 for each growing cycle can be found in Supplementary Fig. 1 as online supporting
31 information for this study). R values above the dotted grey line are significant at $P < 0.05$.
32 $ARain_{hv}$ and $ARain_s$ lines in panel (a) represent the antecedent rainfall series that best correlate

1 with the NDVI series for the Black Grama and Creosotebush Core sites (i.e. time series of
2 precedent rainfall with rainfall accumulation lengths Olr_{hv} and Olr_s , respectively). Reference
3 Olr_{hv} and Olr_s values in panel (b) represent the optimal rainfall accumulation lengths for
4 herbaceous vegetation (57 days) and shrubs (145 days), respectively.

5

6 **Fig. 4.** Principal Component Analysis (PCA) of the NDVI-rainfall correlation coefficients for
7 the herbaceous- and shrub-specific antecedent rainfall series $ARain_{hv}$ and $ARain_s$ (57- and
8 145-day cumulative rainfall series, respectively) and resulting landscape type classification
9 across the 18 km² study area: (a) PCA projection of cases (MODIS pixels), (b) PCA
10 projection of variables (per growing cycle NDVI-antecedent rainfall correlation scores), (c)
11 landscape type classification (GD, grass-dominated, GT, grass-transition, ST, shrub-
12 transition, and SD, shrub-dominated landscapes) as a function of the relationship between
13 PCA Factor 1 and field-estimated vegetation dominance for a reference set of 27 control
14 points, (d) spatial distribution of landscape types in the study area, (e) general view and
15 characteristics of the landscape types. MODIS pixel locations for the ground control points
16 are highlighted in panel (a). Vector labels in panel (b) indicate the dates of the yearly cycles
17 of vegetation growth (April-March). Source for background image in panel (d): 2009 National
18 Aerial Imagery Program (USDA Farm Service Agency).

19

20 **Fig. 5.** NDVI decomposition and transformation into partial Annual Net Primary Production
21 (ANPP) components for herbaceous and shrub vegetation: (a) decomposed NDVI time series
22 of herbaceous and shrub vegetation for the reference SEV LTER Black Grama and
23 Creosotebush Core Sites, (b) relationships between field ANPP and the (per growing cycle)
24 annual integrals of herbaceous and shrub NDVI components for the SEV LTER Core Sites,
25 (c) remote-sensed ANPP estimates against field ANPP determinations (root mean square
26 error, RMSE, and normalized error, NRMSE, of the estimates are shown within the plot) (d)
27 remote-sensed ANPP estimations of herbaceous and shrub vegetation (mean for the 2000-13
28 series) , and (e) herbaceous and shrub contribution to total ANPP (mean for the 2000-13
29 series) across the 18-km² study area.

30

1 **Fig. 6.** Spatiotemporal dynamics of remote-sensed ANPP: **(a)** ANPP differences between
2 landscape types (grass-dominated, grass-transition, shrub-transition, and shrub-dominated
3 landscapes) along 2000-13, **(b)** 2000-13 temporal variations of the shrub contribution to total
4 ANPP for the different landscape types (Pearson's R correlations of shrub ANPP contributions
5 with time). Different letters in panel (a) for each cycle of vegetation growth indicate
6 significant differences between landscape types at $P < 0.05$ (tested using repeated-measures
7 ANOVA and post-hoc Tukey HSD tests). Dotted lines in panel (b) represent weak ($R < 0.40$)
8 correlations. Displayed correlations are significant at $P < 0.05$. Numbers in plot (c) indicate
9 correlation coefficients.

10

11 **Fig. 7.** Scatter plots and correlations (Pearson's R) between remote-sensed ANPP
12 estimations and seasonal precipitation (preceding non-monsoonal, summer monsoonal, and
13 late non-monsoonal rainfall) for the different landscape types (grass-dominated, grass-
14 transition, shrub-transition, and shrub-dominated landscapes): **(a)** herbaceous ANPP, **(b)**
15 shrub ANPP. Solid and dotted lines represent strong ($R \geq 0.40$) and weak ($R < 0.40$)
16 correlations, respectively. Displayed correlations are significant at $P < 0.05$. Numbers within
17 the plots indicate correlation coefficients.

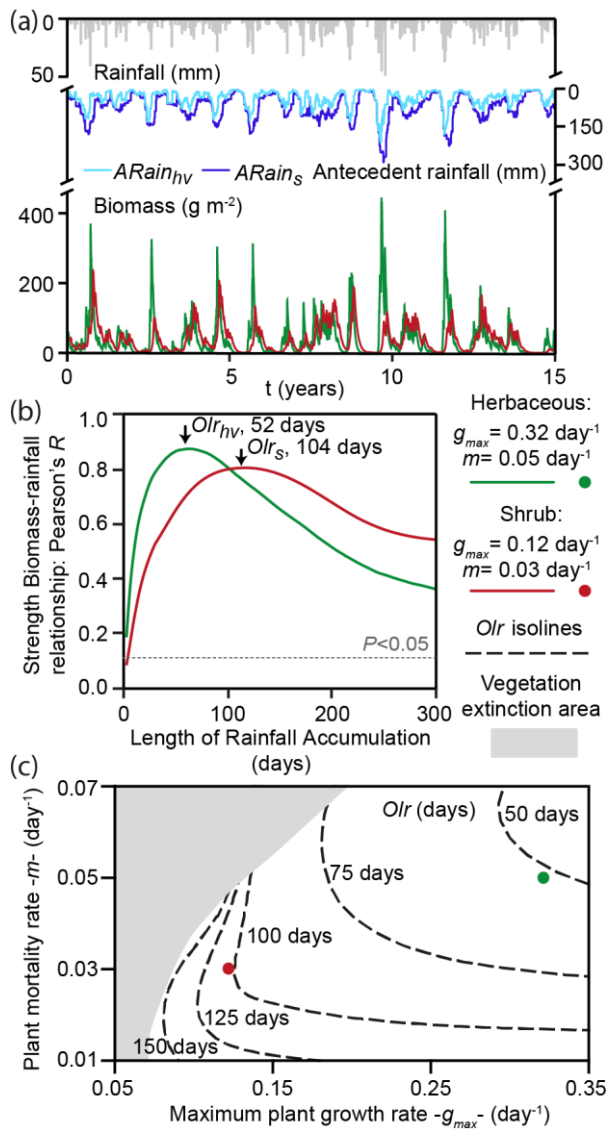


Fig. 1.

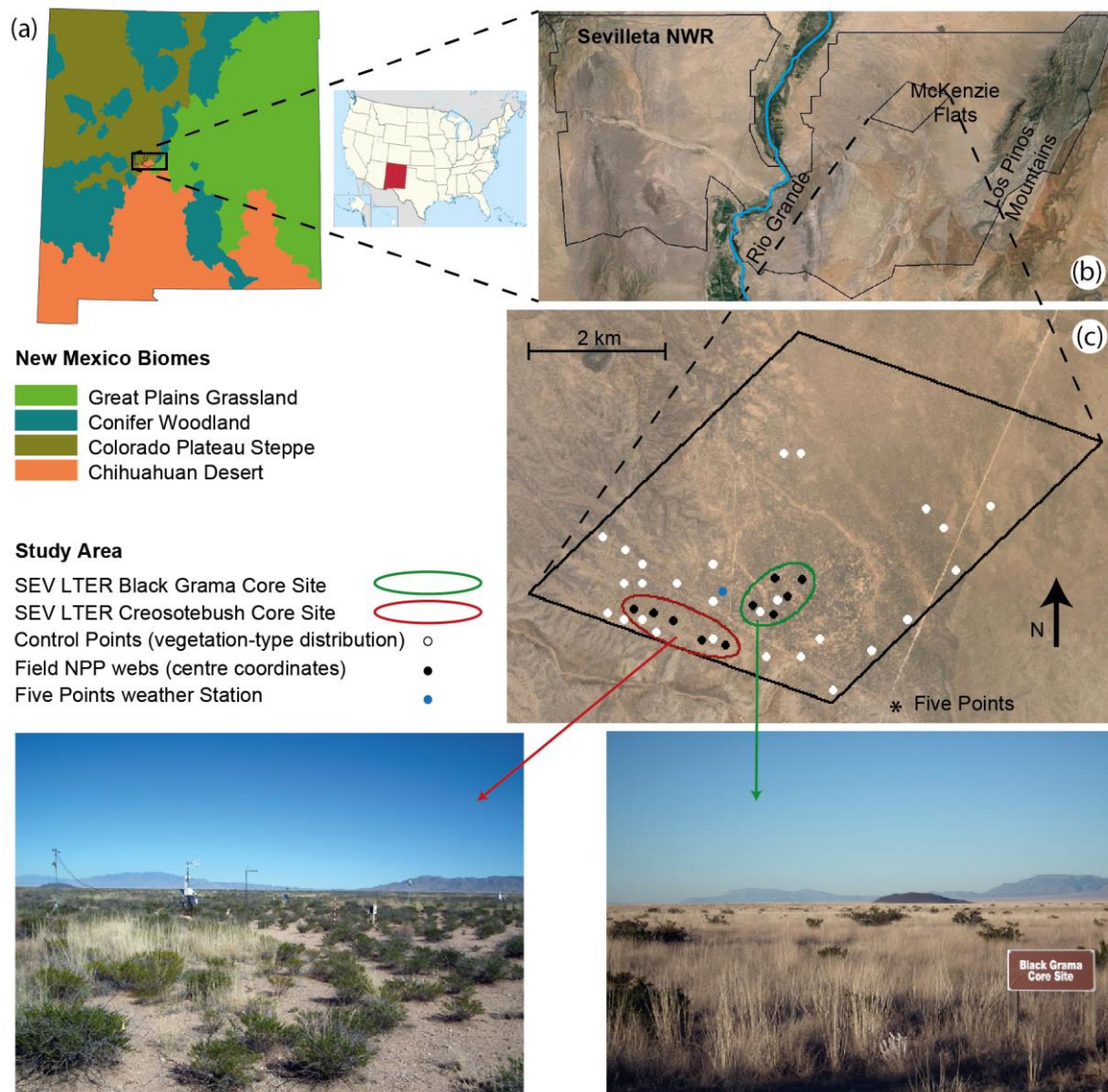


Fig. 2.

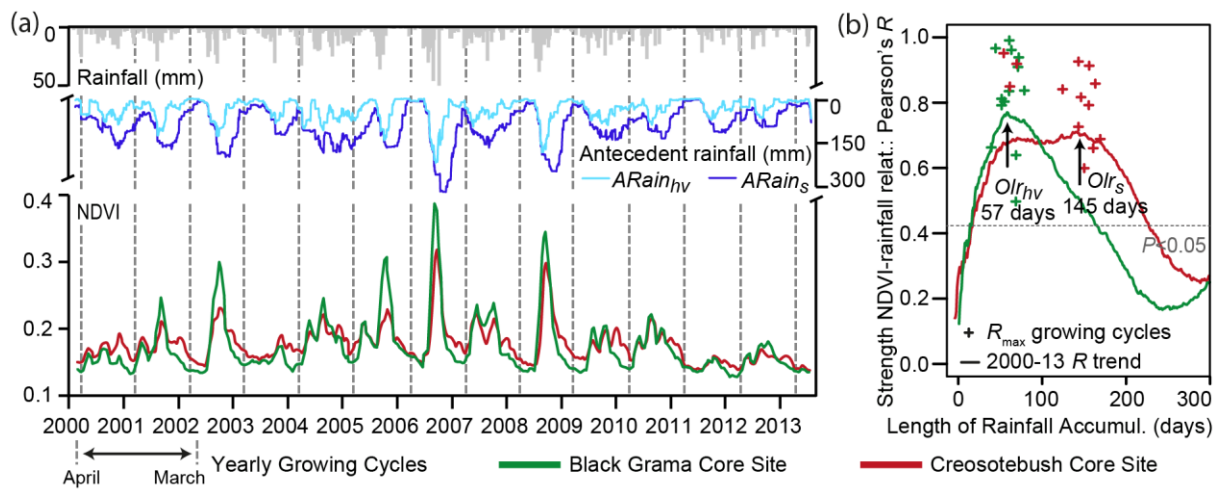


Fig. 3.

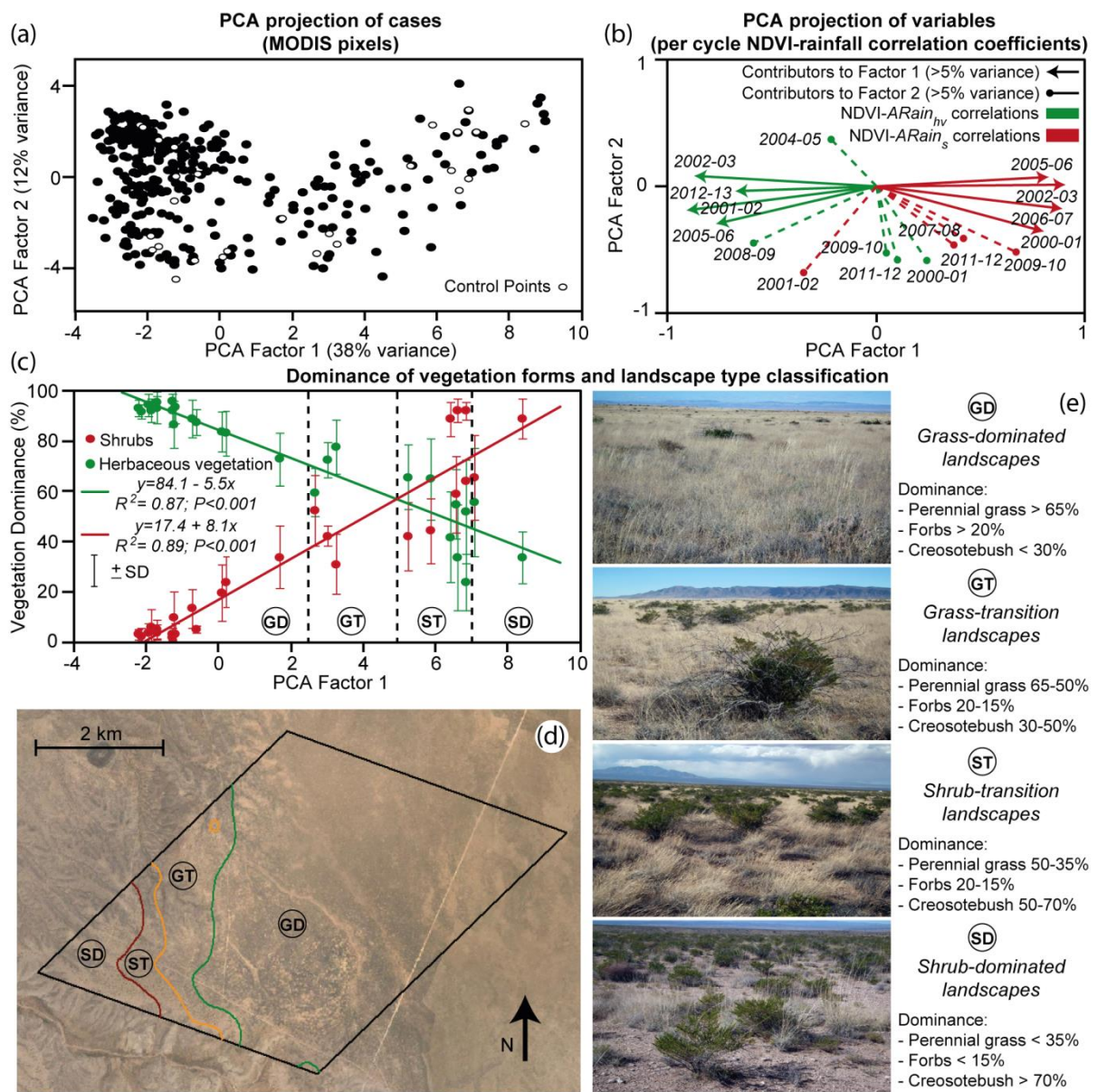


Fig. 4.

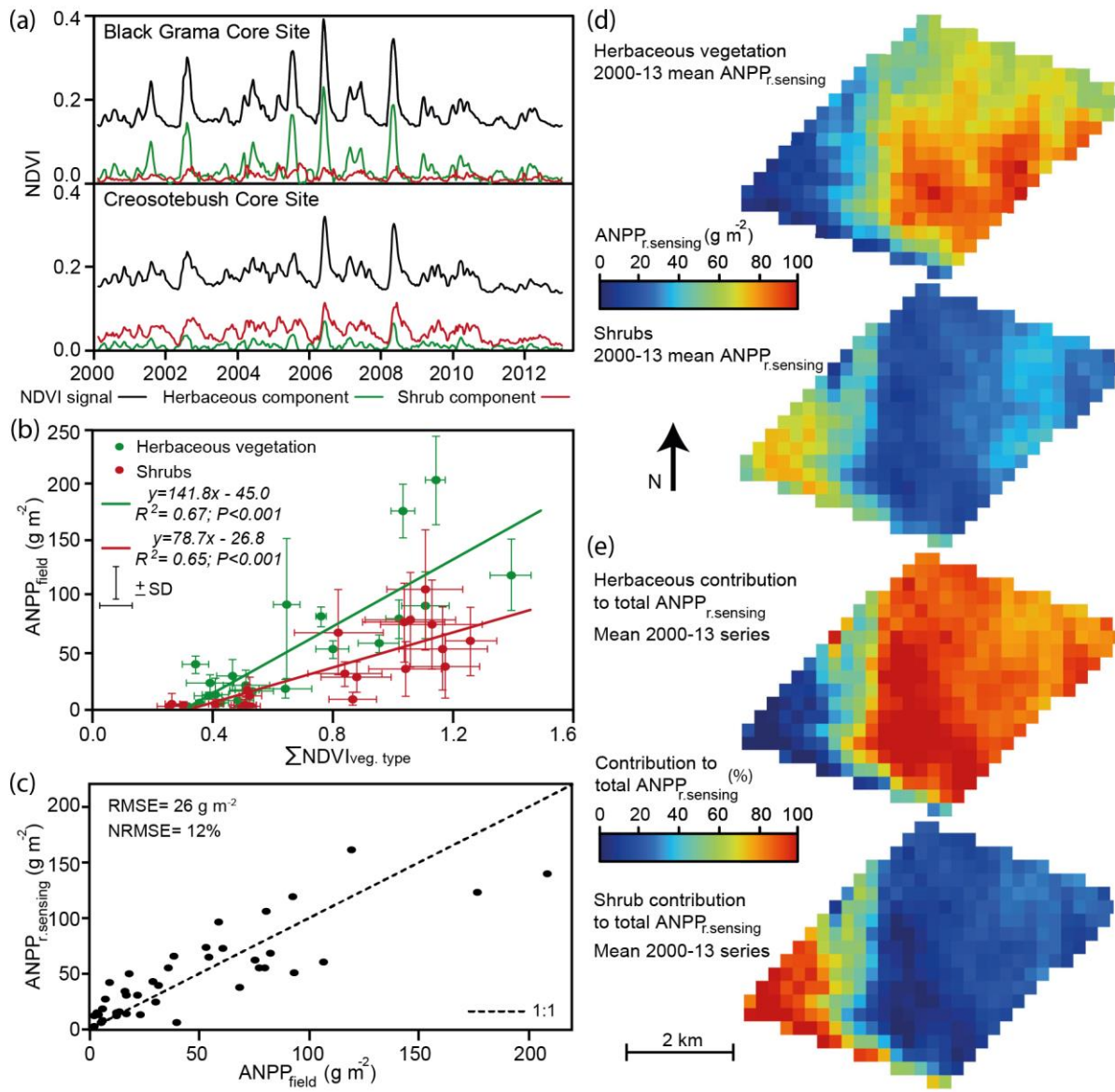


Fig. 5.

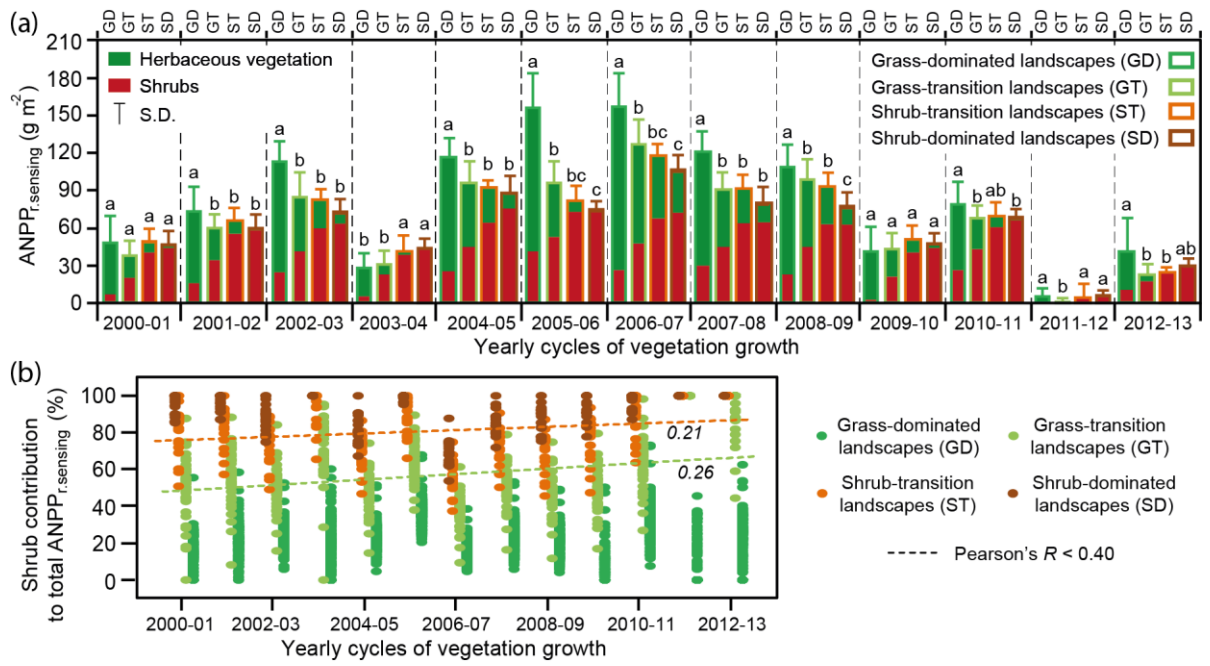


Fig. 6.

1

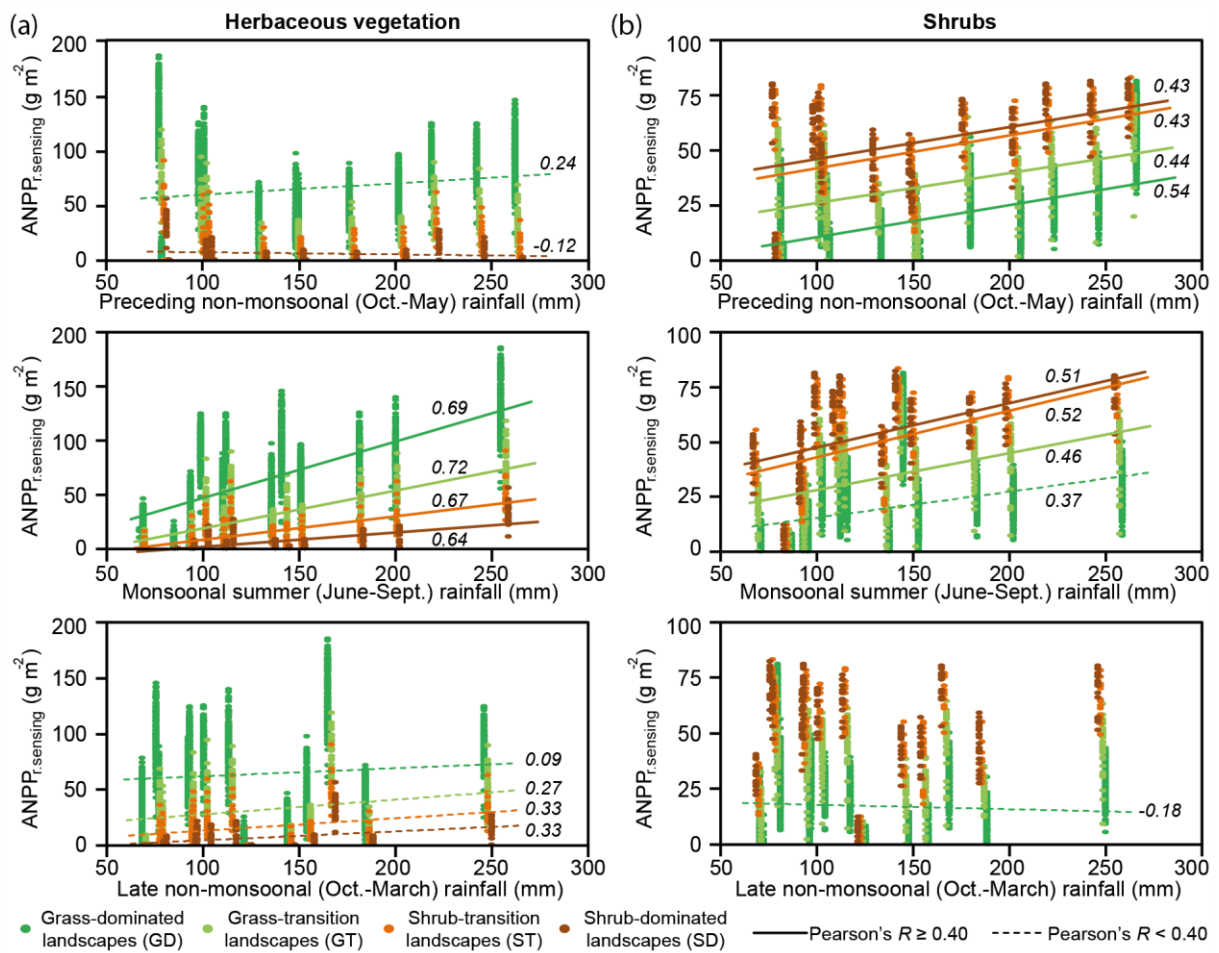


Fig. 7.

1